The Astrophysical Journal, 601:864–884, 2004 February 1

GALACTIC EVOLUTION OF Sr, Y, AND Zr: A MULTIPLICITY OF NUCLEOSYNTHETIC PROCESSES

Claudia Travaglio,[1,2] Roberto Gallino,[3] Enrico Arnone,[3,4] John Cowan,[5] Faith Jordan,[5] and Christopher Sneden[6]

Received 2003 June 27; accepted 2003 October 3

ABSTRACT

In this paper we follow the Galactic enrichment of three easily observed light *n*-capture elements: Sr, Y, and Zr. Input stellar yields have been first separated into their respective main and weak *s*-process components and *r*-process component. The *s*-process yields from asymptotic giant branch (AGB) stars of low to intermediate mass are computed, exploring a wide range of efficiencies of the major neutron source, ^{13}C, and covering both disk and halo metallicities. AGB stars have been shown to reproduce the main *s*-component in the solar system, i.e., the *s*-process isotopic distribution of all heavy isotopes with atomic mass number $A > 90$, with a minor contribution to the light *s*-process isotopes up to $A \sim 90$. The concurrent weak *s*-process, which accounts for the major fraction of the light *s*-process isotopes in the solar system and occurs in massive stars by the operation of the ^{22}Ne neutron source, is discussed in detail. Neither the main *s*- nor the weak *s*-components are shown to contribute significantly to the neutron-capture element abundances observed in unevolved halo stars. Knowing the *s*-process distribution at the epoch of the solar system formation, we first employed the *r*-process residuals method to infer the isotopic distribution of the *r*-process. We assumed a primary *r*-process production in the Galaxy from moderately massive Type II supernovae that best reproduces the observational Galactic trend of metallicity versus Eu, an almost pure *r*-process element. We present a detailed analysis of a large published database of spectroscopic observations of Sr, Y, Zr, Ba, and Eu for Galactic stars at various metallicities, showing that the observed trends versus metallicity can be understood in light of a multiplicity of stellar neutron-capture components. Spectroscopic observations of the Sr, Y, and Zr to Ba and Eu abundance ratios versus metallicity provide useful diagnostics of the types of neutron-capture processes forming Sr, Y, and Zr. In particular, the observed [Sr, Y, Zr/Ba, Eu] ratio is clearly not flat at low metallicities, as we would expect if Ba, Eu and Sr, Y, Zr all had the same *r*-process nucleosynthetic origin. We discuss our chemical evolution predictions, taking into account the interplay between different processes to produce Sr-Y-Zr. Making use of the very *r*-process–rich and very metal-poor stars like CS 22892−052 and CS 31082−001, we find hints and discuss the possibility of a *primary process* in low-metallicity massive stars, different from the "classical *s*-process" and from the "classical *r*-process" that we tentatively define LEPP (lighter element primary process). This allows us to revise the estimates of the *r*-process contributions to the solar Sr, Y, and Zr abundances, as well as of the contribution to the *s*-only isotopes ^{86}Sr, ^{87}Sr, and ^{96}Mo.

Subject headings: Galaxy: abundances — Galaxy: evolution — nuclear reactions, nucleosynthesis, abundances — stars: abundances — stars: AGB and post-AGB

1. INTRODUCTION

In order to reconstruct the solar system composition of the heavy elements beyond Fe, two major neutron-capture mechanisms have been invoked since the classical work by Burbidge et al. (1957): the slow (*s*) process and the rapid (*r*) process. The *s*-process path requires a relatively low neutron density, $n_n < 10^8$ cm^{-3}, and moves along the valley of β stability. This builds up approximately half the nuclides from Fe to Bi, in particular feeding the elements Sr-Y-Zr, Ba-La-Ce-Pr-Nd, and Pb, which define the three major abundance *s*-peaks. The sources for the required free neutrons can be either the reaction ^{22}Ne(α, n)^{25}Mg or ^{13}C(α, n)^{16}O.

Since the first phenomenological analysis, the so-called *classical* analysis (Clayton et al. 1961; Seeger et al. 1965), the *s*-process abundance distribution in the solar system has been recognized as arising from a nonunique site. At least three components have been required: the *main*, the *weak*, and the *strong s*-component (Clayton & Ward 1974; Käppeler et al. 1982; Käppeler, Beer, & Wisshak 1989).

The main *s*-component, accounting for the *s*-process isotopic distribution in the atomic mass number range $90 < A < 208$, was shown to occur in low-mass ($M \lesssim 4\ M_{\odot}$) asymptotic giant branch (AGB) stars during recurrent thermal instabilities developing above the He-burning shell (see Busso, Gallino, & Wasserburg 1999 for a review). The whole He intershell, that is, the region comprised between the H shell and the He shell, becomes convective for a short period of time (the convective thermal pulse [TP]). During the AGB phase, after the quenching of a TP, the convective envelope penetrates below the H-He discontinuity (*third dredge-up* [TDU] episode), mixing to the surface freshly synthesized ^{4}He, ^{12}C, and *s*-process elements. The maximum temperature in the deepest region of the convective TP barely reaches $T = 3 \times 10^8$ K; at this temperature the ^{22}Ne neutron source is marginally activated, and the ^{13}C source plays the major role for the main *s*-component. At TDU, the H-rich envelope and the He

[1] Max-Planck-Institut für Astrophysik, Karl-Schwarzschild-Strasse 1, Postfach 1523, D-85741 Garching bei München, Germany.
[2] Istituto Nazionale di Astrofisica (INAF), Osservatorio Astronomico di Torino, via Osservatorio 20, 10025 Pino Torinese (TO), Italy.
[3] Dipartimento di Fisica Generale, Universitá di Torino, and Sezione INFN di Torino, Via P. Giuria 1, I-10125 Torino, Italy.
[4] Department of Physics and Astronomy, Open University, Walton Hall, Milton Keyes MK7 6AA, UK.
[5] Department of Physics and Astronomy, University of Oklahoma, Room 131 Nielsen Hall, Norman, OK 73019.
[6] Department of Astronomy and McDonald Observatory, University of Texas at Austin, RLM 15.308, Austin, TX 78712.

intershell coming into contact favors the penetration of a small amount of protons into the top layers of the He- and C-rich zones. At hydrogen reignition, protons are captured by the abundant ^{12}C, giving rise to the formation of a so-called ^{13}C *pocket*. Stellar model calculations for the AGB phases by Straniero et al. (1995, 1997) showed that all the ^{13}C nuclei present in the ^{13}C pocket are consumed locally in the radiative layers of the He intershell, before a new TP develops. This provides an *s*-process abundance distribution that is strongly dependent on the initial metallicity (Gallino et al. 1998; Busso et al. 2001).

The weak *s*-component, responsible for a major contribution to the *s*-process nuclides up to $A \simeq 90$, has been recognized as the result of neutron-capture synthesis in advanced evolutionary phases of massive stars. Previous studies (Lamb et al. 1977; Arnett & Thielemann 1985; Prantzos et al. 1990; Raiteri et al. 1991b; The, El Eid, & Meyer 2000) have concentrated on the reaction ^{22}Ne(α, n)^{25}Mg as the major neutron source for this process. The ^{22}Ne neutron source is activated partly in the convective core He-burning and partly in the subsequent convective C-burning shell phase (Raiteri et al. 1991a, 1993). The *s*-process in massive stars is metallicity dependent, since ^{22}Ne is produced from the conversion of CNO nuclei into ^{14}N in the H-burning shell followed by double α-capture on ^{14}N in the early phases of He burning (Prantzos et al. 1990; Raiteri et al. 1992). As we discuss in § 5.3, additional neutron sources, partly of primary origin, may take place in the inner regions of massive stars during convective shell C burning (Arnett & Truran 1969; Thielemann & Arnett 1985; Arnett & Thielemann 1985; Raiteri et al. 1991a) and, more importantly, during explosive nucleosynthesis in the O-rich regions (Hoffmann, Woosley, & Weaver 2001; Heger et al. 2001; Heger & Woosley 2002; Rauscher et al. 2002; Woosley, Heger, & Weaver 2002; Limongi & Chieffi 2003).

Finally, the strong *s*-component was introduced by Clayton & Rassbach (1967) in order to reproduce more than 50% of solar ^{208}Pb, the most abundant Pb isotope. Recent studies by Gallino et al. (1998) and Travaglio et al. (2001b) demonstrated that the role attributed to the strong *s*-component is played by low-metallicity ([Fe/H] < -1.5), low-mass AGB stars.[7]

The *r*-process, however, takes place in an extremely neutron-rich environment in which the mean time between successive neutron captures is very short compared with the time to undergo a β-decay. Supernovae are currently believed to be the site of the *r*-process. However, there have been many attempts to define the right physical conditions for the *r*-process to occur (e.g., Hillebrandt 1978; Mathews & Cowan 1990; Woosley et al. 1994; Wheeler, Cowan, & Hillebrandt 1998). Three possible sites have been discussed in recent works. The first possibility relies on neutrino-powered winds of a young neutron star (Duncan, Shapiro, & Wasserman 1986; Woosley et al. 1994; Takahashi, Witti, & Janka 1994). Recently, Thompson, Burrows, & Meyer (2001) argued that it may be difficult to achieve the necessary high entropy and short timescales in the ejecta in order to reproduce the solar system *r*-process abundance distribution. A second possibility is related to the merging of two neutron stars in a binary system and has been examined by Freiburghaus et al. (1999). However, Qian (2000) argued that the predicted amount of *r*-process ejecta in metal-poor stars would be too high in *r*-elements with $A < 130$ and with $A > 130$ as compared with spectroscopic abundances of metal-poor stars and that the event rate would be too low. The third possibility relies on asymmetric explosions of massive stars and jetlike outflows in the nascent neutron star (Leblanc & Wilson 1970; Cameron 2001, 2003). Each of these proposed sites faces major problems, including reaching the required physical conditions without ad hoc assumptions to produce a satisfactory fit to the solar system *r*-process pattern. Hence, the stellar source for *r*-process abundances is still a matter of debate. Moreover, it has been suggested that at least two different supernova sources are required for the synthesis of *r*-process nuclei below and beyond the neutron magic number $N = 82$ (Wasserburg, Busso, & Gallino 1996; Sneden et al. 2000a; Qian & Wasserburg 2001).

Neutron-capture elements observed in Population II field stars are generally interpreted in an observational framework developed more than 20 years ago. Spite & Spite (1978) first demonstrated that observations of Ba (a predominantly, 80%, *s*-process element in solar system material) and Eu (an *r*-element, 95%, in the solar system) exhibit a nonsolar abundance pattern in unevolved halo stars, with [Eu/Ba] > 0. This was interpreted by Truran (1981) as evidence of an *r*-process nucleosynthesis signature at low metallicities, with little evidence for *s*-process contributions. Observational support for this view has grown in both large-sample surveys (e.g., Gilroy et al. 1988; McWilliam et al. 1995) and detailed analyses of several ultra–metal-poor ([Fe/H] $\lesssim -2.5$) *r*-process–rich stars (e.g., Sneden et al. 2000a; Westin et al. 2000; Hill et al. 2002). The abundances of the heavier *n*-capture elements ($Z \geq 56$) in such stars often are an excellent match to a scaled solar system *r*-process distribution (e.g., Cowan et al. 2002), but *n*-capture abundances of lighter elements below Ba often show significant departures from this distribution. It is not obvious how the observed abundances of the lighter *n*-capture elements in metal-poor stars evolve to those seen in the solar system and in Population I stars.

A detailed *r*- and *s*-process decomposition can be obtained for the solar system, based on the experimental knowledge of neutron-capture cross sections and on the isotopic analysis of meteoritic samples that best represent the protosolar nebula composition. Unfortunately, the solar system composition only provides a single data point in the time evolution of *n*-capture elements in the Galaxy. Investigations into the chemical composition of matter at different epochs can only be accomplished through high-resolution stellar spectroscopic abundance studies. Although the correlation of metallicity with time is hardly perfect, stars with subsolar metallicities are tracers of the chemical compositions of the gas at different times of evolution of the Galaxy. Elemental *n*-capture abundances of field Galactic stars at different metallicities show two main characteristics: (1) an average trend to lower [X/Fe] with decreasing [Fe/H] and (2) a dispersion in [X/Fe] that increases with decreasing [Fe/H]. Theorists have argued that the large dispersions arise from local chemical inhomogeneities in the interstellar medium of heavy elements (in particular Ba, Eu, and Sr), as a result of incomplete mixing of the gas in the Galactic halo (see Tsujimoto, Shigeyama, & Yoshii 1999; Ikuta & Arimoto 1999; Raiteri et al. 1999; Argast et al. 2000, 2002; Travaglio, Galli, & Burkert 2001a).

Spite & Spite (1978) were the first to find observational evidence of a trend of declining [Ba/Fe] and [Y/Fe] below [Fe/H] ~ -2. Unfortunately, their sample of 11 stars was too small to find those rarer stars with supersolar *n*-capture abundances or to detect the intrinsic dispersion in these ratios. The

[7] In this paper we follow the usual convention of identifying overall metallicity with the stellar [Fe/H] value, following the standard notation that $[X/Y] \equiv \log_{10}(N_X/N_Y)_{star} - \log_{10}(N_X/N_Y)_{\odot}$.

earliest evidence for a dispersion at low metallicity came from Griffin et al. (1982), who found very strong Eu lines in the halo star HD 115444 ([Fe/H] ~ -3), subsequently confirmed by the studies of Gilroy et al. (1988), Sneden et al. (1998), and Westin et al. (2000). Other similar well-known examples are stars extremely rich in *r*-process elements with respect to a solar-scaled composition at the observed [Fe/H], like CS 22892−052 (Sneden et al. 2000a, 2003 and references therein), CS 31082−001 (Cayrel et al. 2001; Hill et al. 2002), or stars of comparable metallicity but showing a much lower *n*-capture element enhancement, like HD 122563 (Westin et al. 2000). Other well-observed stars are BD +17°3248 (Cowan et al. 2002) and CS 22949−037 (Depagne et al. 2002). Studies by Gilroy et al. (1988), Ryan et al. (1991, 1996), Gratton & Sneden (1988, 1994), McWilliam et al. (1995), McWilliam (1998), and more recently Burris et al. (2000), Fulbright (2000), and Johnson & Bolte (2002) have found dispersions in *n*-capture element/Fe ratios of more than a factor of 100 from star to star at a given metallicity.

In this paper we study the Galactic chemical evolution (GCE) of Sr, Y, and Zr. The paper is organized as follows: In § 2 we focus on the Sr-Y-Zr production by AGB stars at different metallicities. In § 3 we briefly review the GCE model adopted and our *r*-process assumptions. In § 4 we present our collection of spectroscopic abundances in field stars at different metallicities, updated from the recent literature. The unique compositions of some of the stars of our sample will be discussed. In § 5 we first discuss how the main *s*-process nucleosynthesis in AGB stars reproduces a major fraction of the solar isotopic compositions of Sr-Y-Zr by following their enrichment throughout the Galactic history. We then examine the minor role played by the weak *s*-process in massive stars to the solar system inventory of the first *s*-peak abundances. Both the main and the weak *s*-processes do not affect the heavy-element abundances of unevolved stars at low metallicities. However, we discuss the complex nature of neutron captures occurring in advanced stages of massive stars and the possibility of activation of primary neutron sources during shell C burning or explosive nucleosynthesis in the oxygen-rich regions, not related to the classical *s*- or *r*-process. A general comparison of our *s*-process predictions is then made with spectroscopic observations of Sr, Y, Zr in field stars at different metallicities. In particular, we make use of the spectroscopic observations in extremely *r*-process–rich and very metal-poor stars, like CS 22892−052, to infer the *r*-process fraction of Sr, Y, Zr that is strictly related to the main *r*-process feeding the heavy elements beyond Ba. We also examine very recent spectroscopic observations of heavy elements in dwarf spheroidal galaxies (Shetrone et al. 2001, 2003; Tolstoy et al. 2003), as well as in the globular cluster M15 (Sneden et al. 2000b). In particular, we investigate how they compare with the Galactic trend versus metallicity. In § 6 we show how an extra primary process (not yet fully quantified from the present status of nucleosynthesis models) is needed to fully explain the solar composition of Sr-Y-Zr and in particular their Galactic trend at very low metallicities. Finally, in § 7 we summarize the main conclusions of this work and point out several areas that deserve further analysis.

2. Sr-Y-Zr PRODUCTION BY AGB STARS AT DIFFERENT METALLICITIES

We modeled the AGB nucleosynthesis, as in Straniero et al. (1997) and Gallino et al. (1998), with postprocess calculations that make use of stellar evolutionary models with the Frascati Raphson-Newton evolutionary code (FRANEC; see Chieffi & Straniero 1989). We computed stellar yields for *s*-process elements in AGB stars injected in the interstellar medium by mass-loss winds from stars of different masses. This has been done for both Galactic halo and disk metallicities and for a wide range of ^{13}C pocket efficiencies (see Travaglio et al. 1999, 2001b for applications of these techniques to heavier *n*-capture elements, with $Z \geq 56$). The cumulative He intershell mass dredged up into the envelope and ejected into the interstellar medium is reported in Travaglio et al. (2001b; their Table 1).

In spite of the fact that successful models for the formation of the ^{13}C pocket have been advanced (Hollowell & Iben 1988; Herwig et al. 1997; Langer et al. 1999; Cristallo et al. 2001), the mass involved and the profile of the ^{13}C pocket must still be considered as free parameters, given the difficulty of a sophisticated treatment of the hydrodynamical behavior at the H/He discontinuity during each TDU episode. However, a series of constraints have been obtained by comparing spectroscopic abundances in *s*-enriched stars (MS, S, C, post-AGB, Ba, and CH stars) at different metallicities with AGB model predictions (see, e.g., Busso et al. 1995, 2001; Abia et al. 2001, 2002 and references therein). These authors conclude that the observations in general confirm the complex dependence of neutron captures on metallicity. The spread observed in the abundance ratio of the Ba-peak elements with respect to the lighter Zr-peak elements requires the existence of an intrinsic spread in the mass of the ^{13}C pocket. The same spread in the ^{13}C concentration has been found to be appropriate to match the *s*-process isotopic signature of heavy elements in presolar grains condensed in circumstellar envelopes of AGB stars (see, e.g., Lugaro et al. 1999, 2003 and references therein).

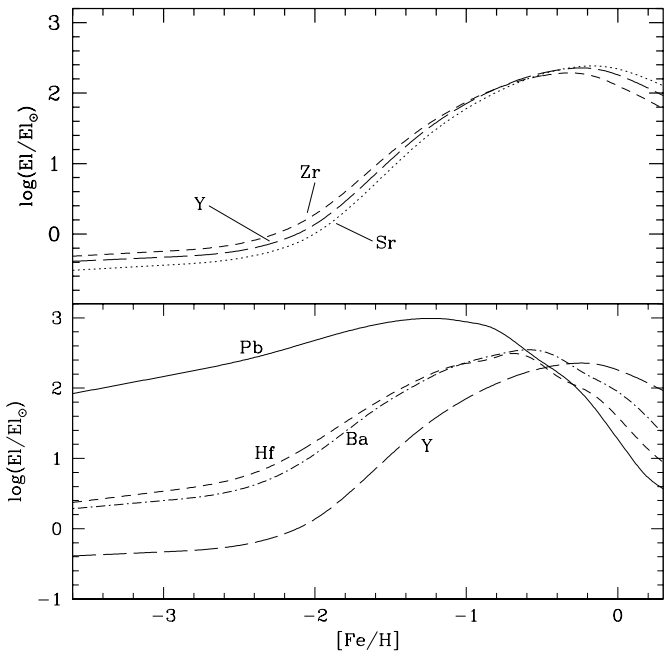

FIG. 1.—Production factors with respect to the solar value in the He intershell material cumulatively mixed by TDU episodes with the envelope of AGB stars of 1.5 $M_{\odot}$ and different metallicities. The production of Sr, Y, Zr is shown in the top panel. In the bottom panel the production of Ba, Hf, and Pb is compared with the Y production. The case ST for the ^{13}C pocket (see text for details) has been adopted.

In our calculations, the intrinsic spread in the *s*-process yields at each metallicity has been modeled parametrically by varying the ^{13}C concentration in the pocket from 0 up to a factor of 1.5 times the "standard" value of $\sim 4 \times 10^{-6}\ M_{\odot}$ of ^{13}C (Gallino et al. 1998; their ST case). Note that a maximum abundance of ^{13}C is expected in the pocket. Indeed, too high a concentration of protons, which may diffuse into the top layers of the pocket, would activate the concurring reaction $^{13}C(p, \gamma)^{14}N$ (with ^{14}N acting as a strong neutron poison).

We show in the top panel of Figure 1 the elemental production factor of Sr, Y, Zr versus [Fe/H] obtained for AGB stars of initial 1.5 $M_{\odot}$ and different metallicities, for the ST choice of the ^{13}C pocket. For comparison we also plot in the bottom panel the elemental production factor of Ba, Hf (an element that also receives a major contribution from the *s*-process), and Pb. In Figure 2 we show the isotopic production factors of Sr (^{86}Sr, ^{87}Sr, ^{88}Sr; *top panel*), Y (^{89}Y; *middle panel*), and Zr (^{90}Zr, ^{91}Zr, ^{92}Zr, ^{94}Zr, ^{96}Zr; *bottom panel*), versus [Fe/H]. Similar trends are obtained for the 3 $M_{\odot}$ case. From this figure it is clear that the *s*-process production in AGB stars, driven by the primary ^{13}C neutron source, gives rise to a wide spectrum of different abundance distributions that are strongly dependent on metallicity. At solar metallicity, AGB stars produce copious amounts of *s*-process elements belonging to the Sr-Y-Zr peak at the neutron magic number $N = 50$. For decreasing [Fe/H], more neutron per Fe seeds are available, thus bypassing the bottleneck at $N = 50$ and progressively feeding elements to the second neutron magic peak (Ba-La-Ce-Nd) at $N = 82$, with a maximum production yield at [Fe/H] ~ -0.6 (see, e.g., the Ba trend of Fig. 1 and Travaglio et al. 1999 for more details). At lower metallicities there are enough neutrons per Fe seed to produce large Pb excesses, in particular the most abundant isotope ^{208}Pb at $N = 126$ (Gallino et al. 1998; Travaglio et al. 2001b). The maximum Pb production occurs at [Fe/H] $= -1$ and then decreases following the decrease of the initial Fe concentration. Note that at very low metallicities there is an important primary contribution to ^{22}Ne. Indeed, the progressive erosion of the bottom of the envelope by the H-burning shell makes some fresh ^{12}C, mixed with the envelope by previous TDU episodes, and converted into ^{14}N and subsequently into ^{22}Ne by double α-capture during the early development of the next TP. The neutrons released by the ^{13}C source in the pocket and by the ^{22}Ne source in the TP are captured by the primary ^{22}Ne and their progenies $^{25, 26}$Mg, which act contemporaneously as neutron poisons and as seeds for the production of the heavy *s*-elements (see discussion in Busso et al. 1999). As a consequence, at very low metallicities the Pb yield levels off instead of further decreasing. This complex behavior of *s*-process production is extremely important in a GCE study.

We also considered AGB stars of intermediate mass (hereafter IMSs), basing our analysis on stellar evolutionary models of 5 and 7 $M_{\odot}$, and extrapolating over the whole metallicity and mass (5–8 $M_{\odot}$) range. Travaglio et al. (1999,

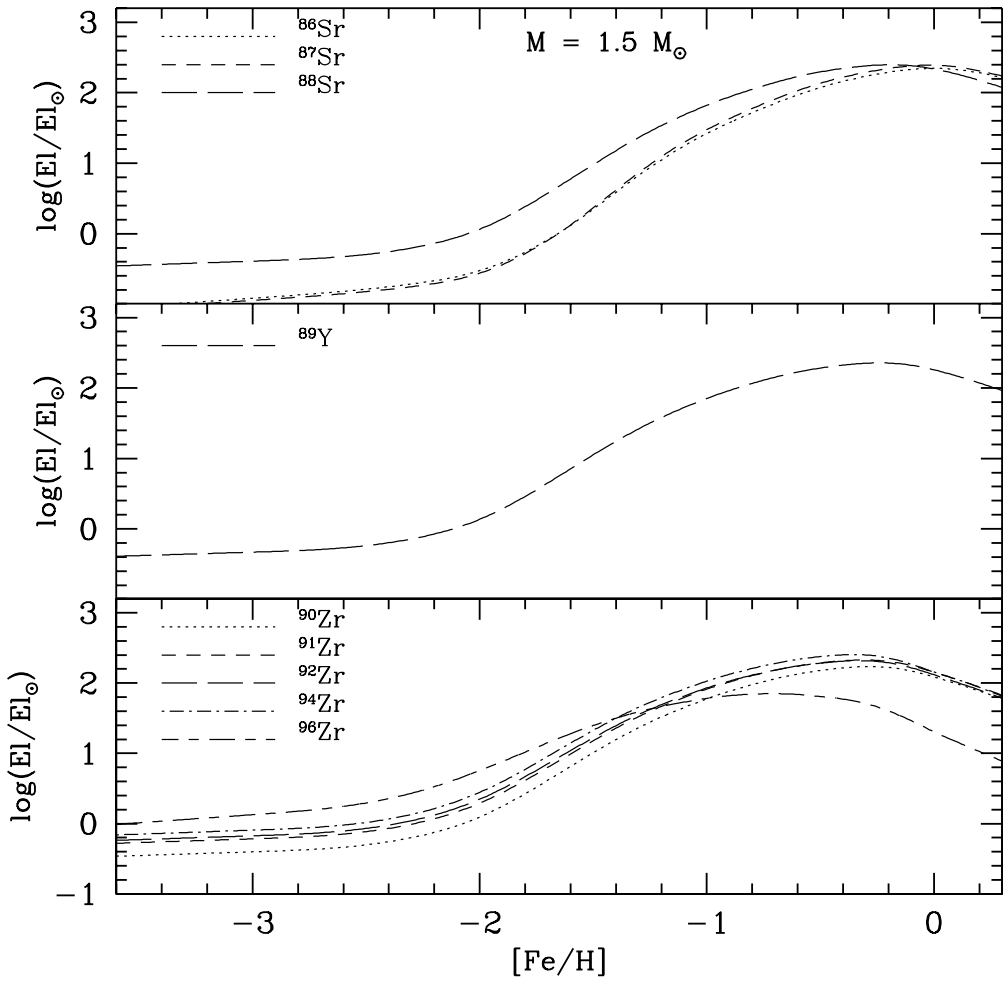

FIG. 2.—Same as Fig. 1, but for the production of Sr (*top*), Y (*middle*), and Zr (*bottom*) isotopes

2001b) discussed the role of IMSs in Ba–Eu and Pb production, concluding that they play a minor role in their Galactic enrichment. Typically in these stars the temperature at the base of the convective envelope reaches $T = 3.5 \times 10^8$ K, allowing ^{22}Ne to release neutrons efficiently via the channel ^{22}Ne(α, n)^{25}Mg (Iben 1975; Truran & Iben 1977). The resulting high peak neutron density ($n_n > 10^{11}$ cm^{-3}) gives rise to an overproduction of a few neutron-rich isotopes, such as ^{86}Kr, ^{87}Rb, and ^{96}Zr, involved in branchings along the *s*-process path and particularly sensitive to the neutron density. The role of IMSs in the light *s*-element production is discussed in § 5.

In Figure 3 we show the production yields for ^{88}Sr obtained for the various assumed ^{13}C pocket efficiencies. Similar trends hold for Y and Zr isotopes. In Figure 3 we also show by a thick line the unweighted average over this spread, the choice adopted for our GCE calculations. With the same technique Travaglio et al. (1999) studied the GCE of the elements from Ba to Eu, and Travaglio et al. (2001b) studied the role of AGB stars in the GCE of Pb and Bi. In § 3 we update the results presented in the previous papers.

3. GALACTIC EVOLUTION OF Sr-Y-Zr: OUR "TOOLS"

Besides the *s*-process yields from AGB stars described in § 2, we need other important tools to discuss the enrichment of Sr-Y-Zr in the Galaxy. First, we outline in § 3.1 the main characteristics of the GCE model that we follow. Since no *r*-process yields are currently available from stellar model calculations, we have introduced them into the GCE model (§ 3.2) under the simple hypothesis of a primary production from Type II supernovae.

3.1. *The GCE Model*

The GCE code for this work has been described in detail by Ferrini et al. (1992). The same model was adopted by Galli et al. (1995) and Travaglio et al. (2001c) to study the evolution of the light elements D, ^{3}He, and ^{7}Li and by Travaglio et al. (1999, 2001b) to study the evolution of the heavy elements from Ba to Pb (see those papers for detailed descriptions; here we only briefly review the basic features). The Galaxy is divided into three zones: halo, thick disk, and thin disk, whose fraction of stars, gas (atomic and molecular), and stellar remnants is computed as a function of time up to the present epoch. Stars are born with the same chemical composition of the gas from which they form. The thin disk is formed from material falling in from the thick disk and the halo. The star formation rate in the three zones is not assumed a priori, but it is obtained as the result of self-regulating processes occurring in the molecular gas phase, either spontaneous or stimulated by the presence of other stars. Stellar nucleosynthesis yields are treated according to the matrix formalism of Talbot & Arnett (1973). The halo phase lasts approximately up to $[\mathrm{Fe/H}] \lesssim -1.5$; the thick-disk phase covers the interval $-2.5 \lesssim [\mathrm{Fe/H}] \lesssim -1$; the thin-disk phase starts at approximately $[\mathrm{Fe/H}] \gtrsim -1.5$.

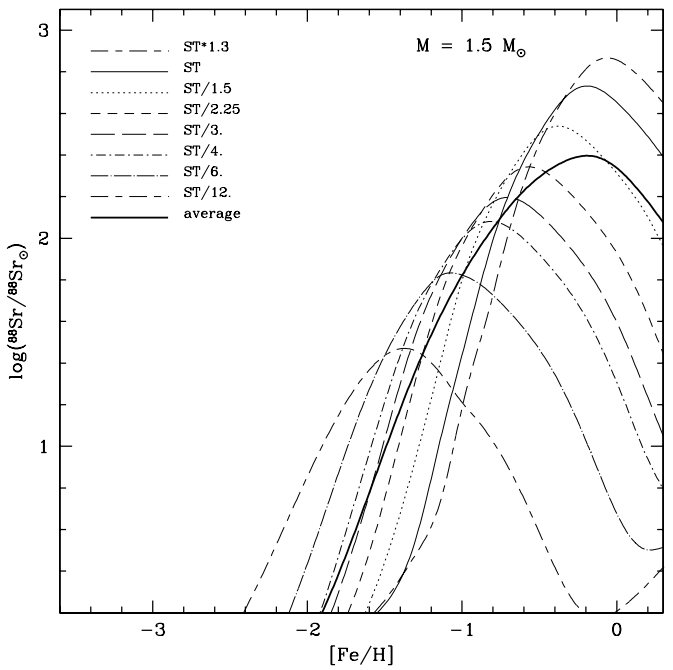

FIG. 3.—Production factors relative to solar of ^{88}Sr in the He intershell material cumulatively mixed with the envelope of a 1.5 $M_\odot$ star by TDU episodes as a function of metallicity, for different assumptions on the ^{13}C concentration in the pocket. The thick solid line represents the unweighted average of all cases shown.

3.2. *The r-Process Assumption*

In halo stars the contribution of AGB stars is too low by far to account for the observed heavy-element abundances. This is essentially due to the long lifetime that low-mass stars spend before reaching the AGB. Moreover, as we discussed in § 2, AGB stars of halo population preferentially produce *s*-isotopes in the Pb peak, with marginal production of elements in the Zr and Ba *s*-peaks.

The almost pure *r*-process signature in halo stars was anticipated by Truran (1981) on theoretical arguments and by Spite & Spite (1978) on observational grounds. For elements from Ba to Pb, our estimate of *r*-process contributions at $t = t_\odot$ has been derived by subtracting the *s*-fractions from the solar abundances (i.e., the *r*-process residuals method). The *r*-process contributions are treated as arising from a primary mechanism occurring in a subset of Type II supernovae, i.e., those in the mass range 8–10 $M_\odot$ (see Wheeler, Cowan, & Hillebrandt 1998). Concerning the *r*-process contribution to elements lighter than barium, and in particular to strontium, yttrium, and zirconium, a more complex treatment is needed, as is discussed in § 5.

4. Sr-Y-Zr ABUNDANCES IN "UNEVOLVED" STARS

In order to compare our model results with observed abundance trends, we selected a sample of spectroscopic observations of Galactic field stars (mostly F and G dwarfs, as well as giants not obviously enriched by local *s*-process production events) at different metallicities, updated with the most recent data available in literature. In Figure 4 we show the data from these surveys in the usual manner, as [Sr/Fe], [Y/Fe], and [Zr/Fe] values in the top, middle, and bottom panels, respectively, plotted versus [Fe/H]. We include results from Spite & Spite (1978), Edvardsson et al. (1993), Gratton & Sneden (1994), McWilliam et al. (1995), McWilliam (1998), Jehin et al. (1999), Tomkin & Lambert (1999), Burris et al. (2000), Fulbright (2000), Sneden et al. (2000a), Westin et al. (2000), Norris, Ryan, & Beers (2001), Mashonkina & Gehren (2001), Mishenina & Kovtyukh (2001), Hill et al. (2002), Cowan et al. (2002), and Depagne et al. (2002). We have also included recent observations in dwarf spheroidal galaxies (Shetrone et al. 2001, 2003), as well as in three giants stars observed in the globular cluster M15 (Sneden et al. 2000b).

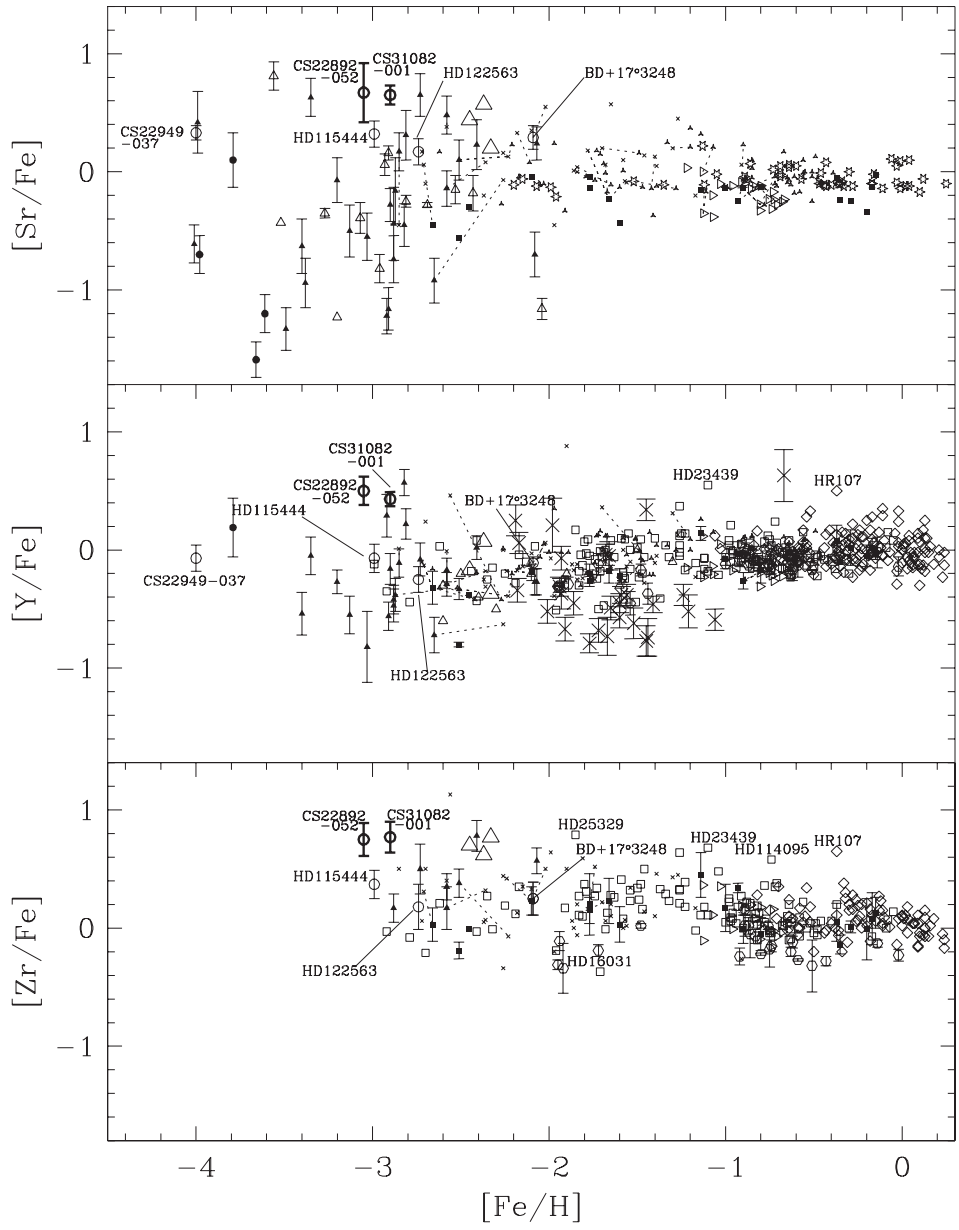

FIG. 4.—Spectroscopic observations of Galactic disk and halo stars at different metallicities for [Sr/Fe] (*top*), [Y/Fe] (*middle*), and [Zr/Fe] (*bottom*) from Spite & Spite (1978; *open triangles*), Edvardsson et al. (1993; *open rhombs*), Gratton & Sneden (1994; *filled squares*), McWilliam et al. (1995) and McWilliam (1998; *filled triangles*), Jehin et al. (1999; *open tilted triangles*), Tomkin & Lambert (1999; *open hexagons*), Burris et al. (2000; *crosses*), Fulbright (2000; *open squares*), Norris, Ryan, & Beers (2001; *filled circles*), Mashonkina & Gehren (2001; *open stars*), and Mishenina & Kovtyukh (2001; *small triangles*). With open circles we indicate "special" metal-poor stars from Westin et al. (2000), Cowan et al. (2002), and Depagne et al. (2002). Two stars, CS 22892−052 (Sneden et al. 2000a) and CS 31082−001 (Hill et al. 2002), are indicated as bold open circles (see text for discussion). Big open triangles are for three stars in M15 (Sneden et al. 2000b; this paper). Big skeletals are for stars in dwarf spheroidal galaxies (Shetrone et al. 2001, 2003). Error bars are shown only when reported for single objects by the authors. The thin dotted line connects a star observed by different authors. The stars indicated with their names are discussed in detail in the text.

In Figure 5 we show for comparison our collection of data for [Ba/Fe] (*top panel*), [Eu/Fe] (*middle panel*), and [Ba/Eu] (*bottom panel*) versus [Fe/H], overimposed with the predicted average Galactic trend for the halo, thick disk, and thin disk according to Travaglio et al. (1999). At disk metallicities the model predictions from AGB stars only are also shown for comparison.

Before applying the same GCE model to the Sr, Y, and Zr data, we pause to alert the reader to some observational uncertainties and limitations. First, the spectral lines all of these elements used in analyses of metal-poor field stars have been subject to extensive laboratory analyses. Therefore, their transition probabilities have small uncertainties. Second, almost all Sr, Y, and Zr abundance results are from ionized transitions of these elements. Thus, abundance intercomparisons among these elements, or comparisons with abundances of rare earth elements (also derived from ionized transitions), have, in most cases, little dependence on choices of effective temperatures or gravities in the various studies included here. However, each of these elements has some particular problems that should be kept in mind.

Strontium abundances are based almost exclusively on the very strong Sr II $\lambda\lambda$4077, 4215 resonance lines. Abundances derived from these transitions are very sensitive to the choice of (in particular) the microturbulent velocity parameter, which can vary from analysis to analysis for the same star. Additionally,

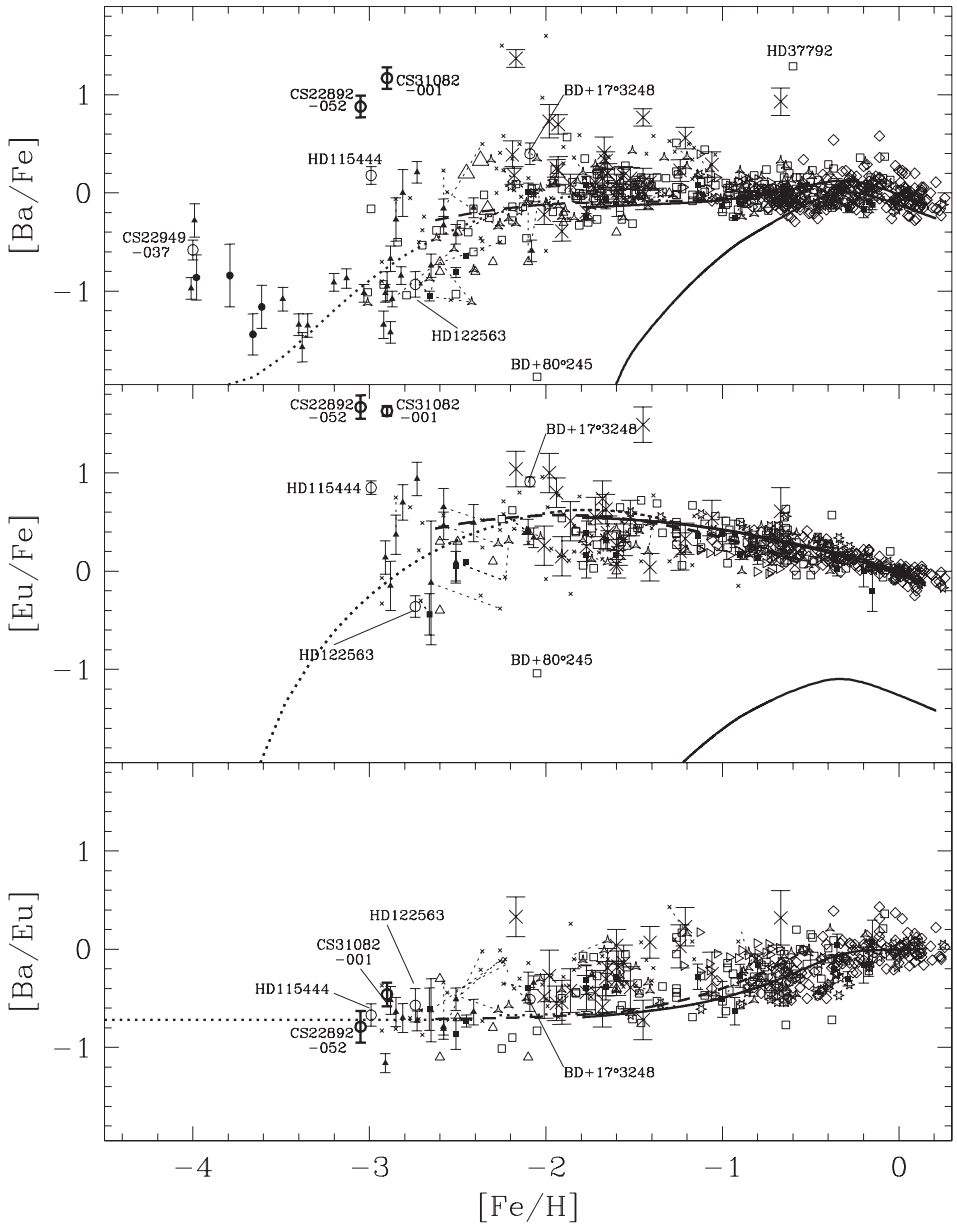

FIG. 5.—Spectroscopic observations of Galactic disk and halo stars at different metallicities for [Ba/Fe] (*top*), [Eu/Fe] (*middle*), and [Ba/Eu] (*bottom*). The symbols are the same as in Fig. 4. The curves represent the total *s*+*r* contribution for the halo (*dotted lines*), thick disk (*dashed lines*), and thin disk (*solid lines*). With a thin disk (*thick solid line*) we show for comparison the AGB *s*-process contribution alone.

these lines suffer some blending from other atomic and molecular transitions, and abundance analyses really ought to be done with synthetic spectrum computations rather than with the more common single-line equivalent width computations. Fortunately, in the rare spectra that have detectable (much weaker) higher excitation Sr II lines and the Sr I λ4607 line, the abundances derived from all Sr features are in reasonable agreement (e.g., Sneden et al. 2003), confirming the reliability of the Sr II resonance lines, given care in their analyses.

Second, yttrium and zirconium abundances usually are derived from a few lines of the ionized species of these elements. None of these lines are usually strong enough for microturbulent velocity uncertainties to be an important source of abundance uncertainty. This comes at a price: such lines of moderate strength in stars of moderate metal deficiency weaken to undetectable levels in the most metal-poor stars; thus, Y and Zr abundances cannot be used to constrain GCE models below [Fe/H] ~ -3.

Abundances of these three elements have been reported for globular cluster giant stars. However, comparisons between field and cluster abundances should be done cautiously because the vast majority of field star abundances are obtained from blue–UV region spectra (where the stronger lines are), while cluster star spectra abundances are based on lines in yellow–red spectral region (where the fluxes are largest in these faint stars). Unfortunately, Sr II lines are few and very weak in the yellow–red, resulting in few Sr abundance determinations in clusters. Furthermore, the results for Y and Zr are so spotty that for the present study we have chosen not to make a detailed comparison with globular clusters. Exceptions are three giant stars in M15 (see discussion below).

However, a few general remarks about heavier *n*-capture elemental abundances in globular clusters are appropriate here. First, note that the cluster metallicity range is $[Fe/H] \gtrsim -2.4$, i.e., there are no ultra–metal-poor Galactic globular clusters. In this metallicity regime the clusters have $[Eu/Fe] \approx +0.4$ ($\sigma = 0.1$), mostly with little star-to-star variations within individual clusters and very small cluster-to-cluster differences (see the review of C. Sneden et al. 2004, in preparation and references therein). This overall Eu enhancement is comparable to the general level in field stars of the same metallicities. Abundances of Ba and La in clusters exhibit more intracluster and intercluster variation, with an unweighted mean value $[Ba, La/Fe] \approx +0.1$ ($\sigma = 0.2$). Combining this ratio with the mean Eu abundance discussed above yields $[Eu/Ba, La] \sim +0.3$ for almost all well-observed globular clusters. This in turn suggests strongly that the heavier *n*-capture elements in globular clusters have been synthesized more heavily by the *r*-process than by the *s*-process, compared with the solar system composition of these elements. Therefore, in general terms, the *n*-capture elements in globular clusters were formed from the same enrichment episodes as was the halo field. There are a few important exceptions to these general statements about globular cluster *n*-capture elements. For example, in M4, a globular cluster with metallicity $[Fe/H] = -1.2$, the *s*-process elements Ba and La are enhanced significantly beyond their nominal levels, e.g., $[Eu/Ba, La] \sim 0.0$ (Ivans et al. 1999). This is very clear evidence for the extra presence of the products of AGB star *s*-process nucleosynthesis, but why this has occurred in M4 and not in most other clusters (e.g., not in the similar-metallicity cluster M5; Ivans et al. 2001) is not well understood. Furthermore, in M15 (one of the most metal-poor clusters, $[Fe/H] \approx -2.4$), a star-to-star scatter is found with a range of 0.5 dex, well beyond observational uncertainties (Sneden et al. 1997; Johnson & Bolte 2002).

Only a few stars of globular clusters have been subjected to a very detailed *n*-capture abundance analysis. As one example, Sneden et al. (2000b) obtained blue-region spectra of three giants in M15. Their representative points are shown in the various figures as big open triangles. The relative *n*-capture abundances from this study showed good agreement with abundances of these elements in so-called *r*-process–rich field stars, i.e., $\langle [Eu/Fe] \rangle \approx +0.80$ and $\langle [Ba/Eu] \rangle \approx -0.85$. The [Eu/Fe] values indicate enhanced *n*-capture elemental abundances in these low-metallicity giants, while the [Ba/Eu] ratios are consistent with an *r*-process solar system abundance value. Both sets of elemental abundance ratios in the globular giants support other studies, based on field halo giants, that demonstrate first the early onset of the *r*-process in the Galaxy and second the dominance of the *r*-process (as opposed to the *s*-process) in the early Galactic synthesis of *n*-capture elements. Yttrium and zirconium (but not strontium) abundances were also derived in these stars, and the mean values were $\langle [Y/Fe] \rangle \approx -0.30$ and $\langle [Zr/Fe] \rangle \approx +0.40$. These values, being both higher and lower than solar, are suggestive of different synthesis histories for Y and Zr, at least, than for the heavier *n*-capture elements, i.e., Ba and Eu.

At typical Galactic disk metallicities, the largest data set for Zr and Y abundances in field stars is that of Edvardsson et al. (1993). The abundances from Gratton & Sneden (1994) and Fulbright (2000) agree well with those numbers at similar metallicities. A first look at these higher metallicity data reveals a puzzle. The average trend of [Zr/Fe] and [Y/Fe] versus [Fe/H] (not enough [Sr/Fe] data are available at high metallicity) is flat within the observational errors. However, at $[Fe/H] \sim -0.6$, the ratio [Zr/Fe] seems to increase slightly with decreasing [Fe/H], while [Y/Fe] seems to decrease slightly with decreasing [Fe/H]. This might suggest differences in the synthesis of these two neighboring elements or perhaps might be related to observational uncertainties. We consider this point later.

We also note the abundance scatter in the Sr, Y, and Zr data. Specifically, starting at $[Fe/H] \lesssim -1.0$ with the Burris et al. (2000) data and becoming even more obvious at halo metallicities ($[Fe/H] \sim -2$), the Sr-Y-Zr abundances are characterized by a large $[X_i/Fe]$ dispersion of $\gtrsim 2$ dex (e.g., McWilliam et al. 1995; Gratton & Sneden 1994; McWilliam 1998). Ultra–metal-poor stars with very large scatter of *n*-capture element abundances are confirmed by recent detailed studies of individual stars (e.g., CS 22892−052, Sneden et al. 2000a; HD 115444 and HD 122563, Westin et al. 2000; CS 31082−001, Hill et al. 2002). This large abundance scatter at the lowest metallicities, declining with increasing [Fe/H], is usually interpreted as an early unmixed Galaxy, with an inhomogeneous composition of the gas in the halo (Gilroy et al. 1988; Burris et al. 2000). This likely occurred because the timescale to homogenize the Galaxy is longer than the early evolution of the halo progenitor massive stars (see, e.g., Ikuta & Arimoto 1999; Raiteri et al. 1999; Argast et al. 2000, 2002; Travaglio et al. 2001a).

In Figures 6 and 7 we have plotted for our collected sample the ratios [Zr/Y], [Sr/Y], and [Sr/Zr] versus [Fe/H] and [Sr, Y, Zr/Ba] versus [Fe/H], respectively. From Figure 4 it appears that Sr at low metallicities shows a much larger scatter with respect to Y and Zr. A theoretical explanation for this effect is difficult. Nevertheless, we notice that at $[Fe/H] < -3$, where the largest scatter for [Sr/Fe] is observed, there are no data available for [Zr/Fe] (as a result of observational limits) and only few data exist for [Y/Fe] (see also discussion in Travaglio et al. 2001a). In stars for which at least two elements among Sr, Y, Zr have been observed (Fig. 6) the relative dispersion is smaller. Only the [Sr/Y] ratio (Fig. 6, *middle panel*) apparently shows a larger dispersion at $[Fe/H] \sim -3$, in particular as a result of two major outliers, HD 200654 ($[Fe/H] = -2.82$, $[Sr/Y] = -1.02$; McWilliam et al. 1995; McWilliam 1998) and CS 22877−011 ($[Fe/H] = -2.92$, $[Sr/Y] = -1.55$; McWilliam et al. 1995; McWilliam 1998). A relatively high [Y/Fe] in both stars seems to be the cause. This is also evident in Figure 7 (*middle panel*) in the plot [Y/Ba] versus [Fe/H]. From the theoretical point of view, the large scatter of Sr in very metal-poor stars may be naturally related to the different explosive properties of stars of different mass and to the consequent different pollution of the local interstellar medium. We recall that the *n*-component operating at very low metallicities is mainly due to explosive nucleosynthesis. Similar characteristics should also affect the *n*-component of Y and Zr. To determine the possibility of an intrinsic scatter in the relative ratios Sr/Y/Zr will require further theoretical study and more observational data.

In Figure 6 the representative points of the two selected very *r*-process–rich stars do not show any appreciable difference with respect to other halo stars in the sample. On the contrary, in Figure 7 the representative points of the two stars are situated at the lower end of the abundance ratio spread, indicating the extremely high *r*-process Ba content. As is discussed in § 5, the interpretation of these ratios contains key information about the stellar origin of these elements.

Some of the stars shown in Figures 4, 5, 6, and 7 appear to deviate from the mean trends enough to warrant further

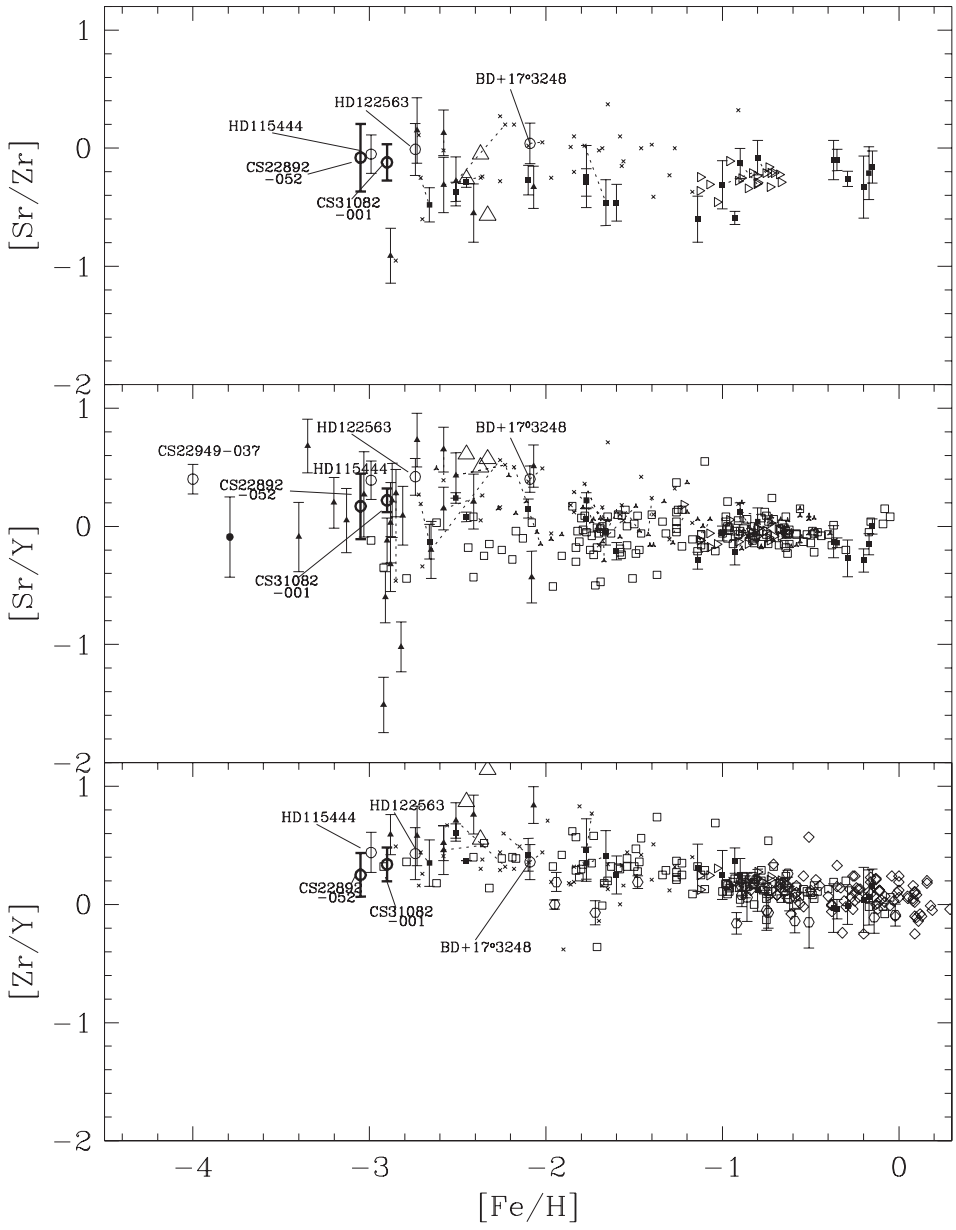

FIG. 6.—Spectroscopic observations of Galactic disk and halo stars at different metallicities for [Sr/Zr] (*top*), [Sr/Y] (*middle*), and [Zr/Y] (*bottom*). The symbols are the same as in Fig. 4. The stars indicated with their names are discussed in detail in the text.

individual attention. Some of these stars are like the F star HR 107 (Edvardsson et al. 1993), which probably is a so-called barium dwarf that has been polluted by mass transfer from a former AGB companion. In this case HR 107 should be taken out of our sample of field stars. Another special star is HD 14095 ([Fe/H] = −0.74; Fulbright 2000); it has a particularly high Zr overabundance, [Zr/Fe] = +0.58, but a solar Y abundance, [Y/Fe] = +0.04. However, J. P. Fulbright (2003, private communication) emphasizes that the Y and Zr abundances for this star are based on very weak lines and should be viewed with caution. The low-metallicity giant HD 110184 ([Fe/H] = −2.56; Burris et al. 2000) also shows high [Y/Fe] and [Zr/Fe] abundances, leading to a suspicion of AGB contamination. In fact, the [Ba/Eu] value given by Burris et al. (2000) is +0.31, much higher than the typical value for this ratio at such metallicity, ordinarily explained by the *r*-process. The same caution holds for HD 105546 ([Fe/H] = −1.27; Burris et al. 2000), BD +54°1323 ([Fe/H] = −1.65; Burris et al. 2000), and BD +17°3248 ([Fe/H] = −2.02; Burris et al. 2000). These stars have high [Sr/Fe] (+0.45, +0.57, +0.55, respectively), but also high [Ba/Eu] ratios (+0.10, −0.10, +0.01, respectively). We also put a warning on BD −12°582 and BD +42°466 (with [Fe/H] = −2.25 and [Fe/H] = −2.00, respectively; Burris et al. 2000). They show a very high [Ba/Fe] ratio (+1.50 and +1.60, respectively), but no other measurements of heavy elements are available (such a high [Ba/Fe] abundance suggests AGB contamination). Finally, we note two dSph stars, Fornax 21 ([Fe/H] = −0.67; Shetrone et al. 2003) and Ursa Minor K ([Fe/H] = −2.17; Shetrone et al. 2001). In both cases their high [Ba/Eu] ratios ([Ba/Eu] = +0.32 and +0.33, respectively) indicate an AGB origin.

5. GALACTIC EVOLUTION OF Sr-Y-Zr: RESULTS

In this section we first discuss the results of the Galactic evolution of Sr, Y, Zr, obtained using the *s*-process yields of

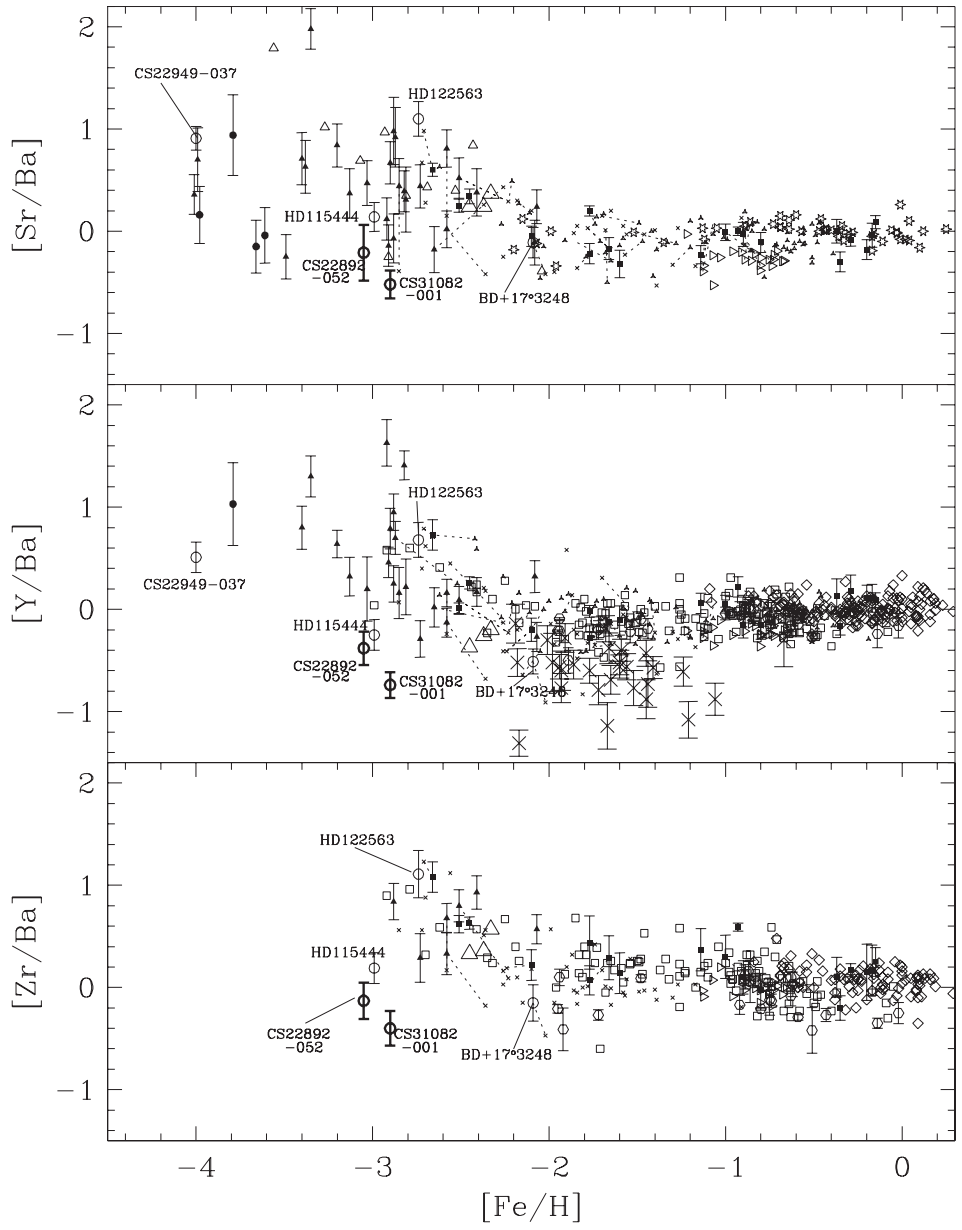

FIG. 7.—Spectroscopic observations of Galactic disk and halo stars at different metallicities for [Sr/Ba] (*top*), [Y/Ba] (*middle*), and [Zr/Ba] (*bottom*). The symbols are the same as in Fig. 4. The stars indicated with their names are discussed in detail in the text.

AGB stars with the unweighted average over the large spread in the ^{13}C pocket efficiencies assumed (see Fig. 3 and the discussion in § 2). An analysis of the properties of the weak *s*-component is then afforded, as it occurs in massive stars in a delicate balance between various nucleosynthetic sources. The weak *s*-component contributes a small fraction to solar Sr and marginally to solar Y and Zr. No weak *s*-contribution is expected in halo stars because of the strong decrease in its efficiency with decreasing metallicity by the effect of the secondary-like nature of the major neutron source in massive stars, ^{22}Ne(α, n)^{25}Mg, and to the strong neutron poison effect of primary isotopes, like ^{16}O, with large abundances. We then deduce the *r*-process isotopic fractions at the epoch of the solar system formation, which enables us to follow separately how the *s*- and *r*-processes evolve in the Galaxy. From the analysis of the chemical composition of peculiar very metal-poor and very *r*-process–rich stars we quantify the primary *r*-process contribution to Sr, Y, and Zr that accompanies the production of the *r*-process characterizing the heavy elements beyond Ba. This small contribution is expected to decrease at very low metallicity, following the generally observed abundance decrease of the heavy neutron-capture elements. The residual fraction of solar Sr, Y, and Zr is of primary nature and is likely produced by all massive stars; it is not strictly related to the classical *r*-process or to the weak *s*-process.

5.1. *s-Process Contribution by AGB Stars at Solar System Formation*

As shown in previous works on this topic (e.g., Gallino et al. 1998; Busso et al. 1999; Travaglio et al. 1999, 2001b), the main *s*-process component is clearly not the result of a "unique" astrophysical process. Instead, it results from the integrated chemical evolution of the Galaxy, mixing into the interstellar medium the output of many different generations of AGB stars, whose yields change with the initial metallicity, stellar mass, ^{13}C pocket efficiency, and other physical properties. This

changes the traditional interpretation of the various *s*-process components. For example, Travaglio et al. (2001b) showed, in the context of the same GCE model adopted here, that at low metallicities Pb (in particular ^{208}Pb) becomes the dominant product of low-mass AGB nucleosynthesis, offering a natural explanation for the strong *s*-component.

The solar abundances of Sr, Y, and Zr from Anders & Grevesse (1989) are listed in Table 1 (second column) together with their uncertainties (1 σ, third column). The resulting Galactic *s*-fractions from AGB stars at the epoch of the solar system formation are listed in the fifth column. They were obtained taking into account the sum of low-mass star (LMS) and IMS yields. As one can see from this table, the contributions from IMSs alone (fourth column) are, in some cases, not negligible. In particular, ^{96}Zr, an isotope originally considered of *r*-process origin (see, e.g., Cameron 1973; Käppeler et al. 1989), receives a substantial *s*-process contribution through the neutron-capture channel at ^{95}Zr if $n_n \gtrsim 3 \times 10^8$ cm^{-3}. For a discussion of the branching effect at ^{95}Zr, see Käppeler et al. (1990). While IMSs do not dominate the present population of AGB stars, they are nevertheless effective in contributing $\sim$10% of solar Sr, Y, Zr, with a much smaller contribution to heavier elements up to Xe, complementing the nucleosynthesis of LMSs.

In Table 1 our corresponding *s*-process expectations for Nb and Mo are also added. The isotope ^{93}Nb is bypassed during the *s*-fluence, but its *s*-process contribution results totally from the radiogenic decay of ^{93}Zr. Consequently, the two elements Zr and Nb share the same origin: the *s*-process contributes approximately the same amount to the solar abundances of each element. Finally, molybdenum also might be included in the Sr-Y-Zr-Nb *s*-peak because of its substantial *s*-process fraction (38% of solar Mo). For this reason, we have tentatively included Mo in Table 1. In the list of isotopes reported in Table 1 we excluded the *p*-only isotopes ^{84}Sr and ^{92}Mo, ^{94}Mo, which are bypassed by the *s*-process. Note that for Mo this corresponds to a contribution of 14% to the solar value. We also excluded the *r*-only ^{100}Mo. We note that ^{86}Sr, ^{87}Sr, and ^{96}Mo are *s*-only isotopes, and from our total *s*-process (main+weak) predictions for the solar composition (Table 1, seventh column), we obtain total contributions of 76%, 70%, and 80%, respectively. Therefore, an additional contribution from a *slow* neutron-capture process is needed to reproduce their solar composition.

The uncertainties in the *s*-fractions depend on the prescriptions for AGB yields and the GCE model, as well as on the uncertainty of neutron-capture cross sections and solar abundances. As for the experimental neutron-capture cross sections, those for the Sr isotopes and for ^{89}Y are fairly well known, at a 5% level or less (Bao et al. 2000; Koehler et al. 2000). A similar precision has been achieved for ^{94}Zr and ^{96}Zr by Toukan & Käppeler (1990), whereas for ^{90}Zr, ^{91}Zr, ^{92}Zr, and ^{93}Zr a higher uncertainty of about 10% is reported in the recent compilation of cross sections by Bao et al. (2000). The latter cross sections are based on the older measurements of Boldeman et al. (1976). A further uncertainty affects the ^{96}Zr *s*-process contribution, which is fed by the neutron channel at ^{95}Zr, whose neutron-capture cross section is based on theoretical estimates only. A reliable determination of these cross sections with improved measurements is highly desirable. In the sixth column we report the contributions to these isotopes from the weak *s*-component, according to the analysis of Raiteri et al. (1993; see discussion in § 5.2). Finally, in the seventh column we report the total *s*-process contributions from AGBs and from the weak *s*-component in massive stars.

In the second column of Table 2 we report the updated predictions from the classical analysis (''classical'' in Arlandini et al. 1999). In the third column we report the *s*-process predictions for the best fit to the main *s*-component (indicated as ''stellar model'' in Arlandini et al. 1999). Those authors

TABLE 1

s-Process Fractional Contributions at $t = t_\odot$ with Respect to Solar System Abundances

	Solar[a]		GCE[b]			
Element	Atom (%)	σ (%)	IMSs (%)	LMSs+IMSs (%)	Weak *s*[c] (%)	TOT *s*[d] (%)
^{86}Sr	9.86	...	8	52	24	76
^{87}Sr	7.00	...	5	54	16	70
^{88}Sr	82.58	...	10	75	7	82
Sr	...	8.1	9	71	9	80
^{89}Y	100	...	7	69	5	74
Y	...	6.0	7	69	5	74
^{90}Zr	51.45	...	6	53	2	55
^{91}Zr	11.22	...	18	80	3	83
^{92}Zr	17.15	...	15	76	3	79
^{94}Zr	17.38	...	9	79	2	81
^{96}Zr	2.80	...	40	82	0	82
Zr	...	6.4	10	65	2	67
^{93}Nb	100	...	12	67	2	69
Nb	...	1.4	12	67	2	69
^{95}Mo	15.92	...	4	39	1	40
^{96}Mo	16.68	...	8	78	2	80
^{97}Mo	9.55	...	6	46	1	47
^{98}Mo	24.13	...	6	59	1	60
Mo	...	5.5	4	38	1	39

[a] Anders & Grevesse 1989.
[b] This paper.
[c] Raiteri et al. 1993.
[d] Total from *s*-process: main *s* plus weak *s*.

TABLE 2

s-Process Fractional Contributions at $t = t_{\odot}$ with Respect to Solar System Abundances

Element	Main *s*		
	Classical Analysis[a] (%)	Stellar Model[a] (%)	GCE[b] (%)
^{86}Sr	68	47	52
^{87}Sr	74	50	53
^{88}Sr	94	92	75
Sr	90	85	71
^{89}Y	106	92	68
Y	106	92	69
^{90}Zr	68	72	56
^{91}Zr	100	96	88
^{92}Zr	108	93	82
^{94}Zr	116	108	84
^{96}Zr	51	55	101
Zr	82	83	65
^{93}Nb	100	85	67
Nb	100	85	67
^{95}Mo	55	55	39
^{96}Mo	116	106	78
^{97}Mo	68	59	46
^{98}Mo	90	76	59
Mo	54	50	38

[a] Arlandini et al. 1999.
[b] GCE *s*-process fraction LMSs+IMSs.

obtained this result with AGB models with masses from 1.5 to 3 $M_{\odot}$, a metallicity of [Fe/H] = −0.3, and with the ST choice for the ^{13}C pocket. A comparison with the results shown in Table 2 makes clear that, even using the same updated neutron-capture network, the classical analysis does not allow any *r*-process residuals for Y (at odds with spectroscopic observations of low-metallicity stars). For the light *s*-elements, both the classical analysis and the stellar model by Arlandini et al. (1999) give different prescriptions with respect to the ones obtained by integrating AGB *s*-yields over metallicity in the framework of the GCE model.

In Table 3 we report our GCE predictions for all elements from Co up to Mo, taking into account the weak *s*-process from Raiteri et al. (1992) (second column), our LMS and IMS predictions separately (third and fourth columns), and the total predictions from AGB stars (fifth column). Finally, our predictions for the total *s*-process (IMS+LMS+weak *s*-component) fractions of solar abundances are reported in the sixth column. From Table 3 we see that solar Kr and Rb have an *s*-fraction of ∼50%. Those two elements belong to the first *s*-peak at $N = 50$. In addition, solar gallium and germanium have a contribution from the *s*-process of ∼50%, while for selenium the *s*-process is responsible for ∼40%. The major *s*-component that contributes to the solar abundance of these three elements comes from the metallicity-dependent weak *s*-process. We also notice that among the two easily observable and nearby elements copper and nickel, only copper is affected by the *s*-process at ∼30%. This is mostly due to the weak *s*-process in massive stars. Nickel is almost unaffected by the *s*-process (see Raiteri et al. 1992; Matteucci et al. 1993; Mishenina et al. 2002; Simmerer et al. 2003). In Figure 8 we show (*filled circles*) the Galactic chemical contribution at the epoch of the solar system formation of elements in the atomic number range $Z = 6$–82, taking into account AGBs of low and intermediate mass. For the light elements below Fe, there is a small *s*-process AGB contribution to P (2.1%) and Sc (1.6%). In addition, AGBs make large contributions to the isotopes ^{12}C (29% solar) and ^{22}Ne (44% solar), leading to total element fractions of 29% for solar carbon and 3.5% for solar neon (Arnone et al. 2003). As for nitrogen, we only considered the yields during the advanced TP-AGB phase when the star suffers thermal pulses and TDU episodes. Here all the ^{14}N nuclei produced in the H-burning shell by the full operation of the HCNO cycle are subsequently converted by double α-capture into ^{22}Ne. However, a major contribution to solar N comes from LMSs in the red giant phase as a result of the first dredge-up. During this phase, material of the inner radiative

TABLE 3

s-Process Contribution at $t = t_{\odot}$

Element	Massive Stars[a] Weak *s* (%)	AGB Stars[b]			Total *s* Weak *s* + Main *s* (%)
		LMSs (%)	IMSs (%)	Total AGB (%)	
Co	6	1	2	3	9
Ni	1	0	0	0	1
Cu	22	2	3	5	27
Zn	8	2	1	3	11
Ga	44	7	4	11	55
Ge	43	8	4	12	55
As	17	5	3	8	25
Se	25	9	5	14	39
Br	11	9	6	15	26
Kr	19	17	12	29	48
Rb	14	18	21	39	53
Sr	9	62	9	71	80
Y	5	62	7	69	74
Zr	2	55	10	65	67
Nb	2	55	12	67	69
Mo	1	34	4	38	39

[a] Raiteri et al. 1992.
[b] This paper.

zones is mixed with the surface by the extension of the convective envelope, and proton captures convert about $\frac{1}{3}$ of the initial ^{12}C into ^{14}N. Further substantial contribution from the nitrogen content in the Galaxy derives from the operation of the so-called cool bottom process in low-mass AGBs and of the hot bottom process in IMSs (see discussion in Busso et al. 1999 and references therein). Both contributions have not been considered here.

For elements beyond Fe and up to Zn, AGBs make minor *s*-process contributions to Co (2.7%), Cu (5.2%), and Zn (2.6%). For comparison we also show, for elements from Sr up to Bi, the *s*-process predictions for the best fit to the main *s*-component from Arlandini et al. (1999): from the stellar model (*open squares*; see also Table 2) and the updated predictions by the classical analysis (Arlandini et al. 1999; see also Table 2). It is clear from this figure that in the Ba–Eu region, and up to Tl, the GCE model agrees quite well with the Arlandini et al. (1999) stellar model. This is mainly due to the fact that the metallicity region around $[\mathrm{Fe/H}] = -0.3$, corresponding to the stellar models adopted by Arlandini et al. (1999), is also the metallicity where the higher AGB production of elements between Ba and Eu and up to Tl occurs (Travaglio et al. 1999). The discrepancy between the predictions for Pb and Bi (see Travaglio et al. 2001b for a detailed discussion) from the classical analysis and from the stellar model is a clear indication that neither a unique AGB nor the classical analysis is able to explain the main *s*-component in the solar system. As a matter of fact, the main *s*-component is the outcome of different generations of AGB stars prior to the solar system formation.

5.2. *The Weak s-Process and Its Contribution to Solar* Sr, Y, Zr

Neutron-capture processes in massive stars at different metallicities play a role in the Galactic production of Sr, Y, and Zr. We intend to discuss in this section some relevant points of this problem.

As we already noted in § 1, the reaction ^{22}Ne(α, n)^{25}Mg represents the major neutron source for the weak *s*-process in massive stars. It takes place partly in the final phases of core He burning (near He exhaustion), when the central temperature rises up to 3.5×10^8 K, and partly in the subsequent convective C-burning shell at a much higher temperature (around 1×10^9 K). There, a copious release of α-particles comes out from the major reaction channel $^{12}\mathrm{C} + ^{12}\mathrm{C} \rightarrow ^{20}\mathrm{Ne} + \alpha$. Consequently, this *s*-process production has a complex dependence on the initial mass. Indeed, during core He burning, ^{22}Ne is less consumed in the less massive stars, and thus a major fraction is available for the subsequent convective shell C-burning phase. In the more massive stars, almost all ^{22}Ne has

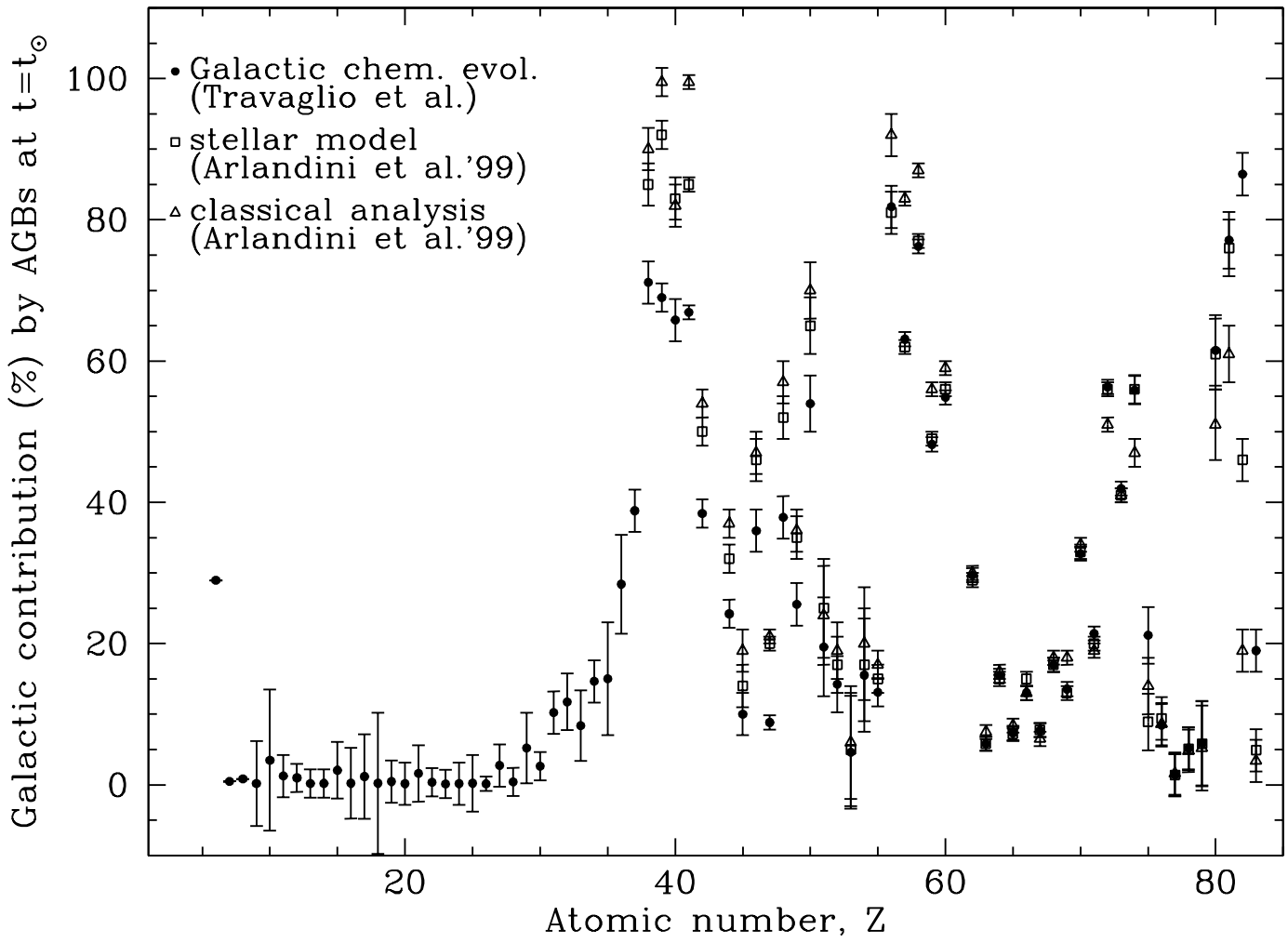

FIG. 8.—Galactic contribution by AGB stars at the epoch of the solar system formation. Three different models have been considered: the classical analysis (Arlandini et al. 1999; *open triangles*), stellar model (Arlandini et al. 1999; *open squares*), and GCE (Travaglio et al. 1999, 2001b; this paper; *filled circles*). For light elements below Fe, there is a small *s*-process AGB contribution to P (2.1%) and Sc (1.6%). AGBs are responsible for 29% and 3.5% of the solar carbon and neon, respectively (Arnone et al. 2003). For elements beyond Fe and up to Zn, there is a minor *s*-process contribution from AGBs to Co (2.7%), Cu (5.2%), and Zn (2.6%).

been consumed already by core He exhaustion, and a saturation in the neutron exposure is reached (Prantzos et al. 1990). During convective core He burning, the neutron density barely reaches 1×10^6 cm^{-3}. In contrast, at the beginning of convective shell C burning the neutron density shows a sharp exponential decline from an initial very high value, of $\sim 1 \times 10^{11}$ cm^{-3} (Arnett & Truran 1969; Raiteri et al. 1991a, 1993), as a result of the early release of α-particles.

Previous analyses of the weak *s*-component (e.g., Couch, Schmiedekamp, & Arnett 1974; Lamb et al. 1977; Prantzos et al. 1990; Raiteri et al. 1991b, 1992, 1993) provided a decreasing *s*-process contribution from massive stars with increasing atomic number, on the order of 70% for the *s*-only ^{70}Ge and of 30% for the *s*-only ^{76}Se. As for Kr, the extreme temperature dependence of the mean life of ^{79}Se favors the production of the *s*-only ^{80}Kr (this isotope is mostly produced, by 80%, in massive stars). In addition, the *s*-only ^{82}Kr receives an important contribution (50%) from the weak *s*-component. Concerning the Sr isotopes, the branching effect at ^{85}Kr favors the *s*-only ^{86}Sr and ^{87}Sr, whose solar abundances are produced by about 20% from the weak *s*-process. The low overall neutron exposure almost stops the *s*-fluence at the neutron magic ^{88}Sr. This isotope receives only a $\sim$5% contribution from the weak *s*-process. From ^{89}Y on, the weak *s*-process contribution is marginal.

It should be clear from the previous considerations that the classical analysis of the weak *s*-process, which typically requires a constant temperature and constant neutron density and an unknown distribution of neutron exposures, is not suitable at all in approximating the weak *s*-process occurring in massive stars.

In massive stars a general note of caution needs to be addressed to the sensitivity of the predicted abundances of nuclei at neutron magic $N = 50$ and on the uncertainty in the cross section of several lighter isotopes for which only theoretical estimates are given, including ^{62}Ni, $^{72, 73}$Ge, and $^{77, 78}$Se. Moreover, many cross sections of stable isotopes from Fe to Sr still have uncertainties of at least 10%. In addition, the temperature dependence of the cross section of several isotopes shows strong departures from the usual $1/v$ law, among them ^{56}Fe, ^{61}Ni, ^{63}Cu, ^{67}Zn, ^{71}Ga, ^{73}Ge, ^{75}As, and all the Kr isotopes.

Finally, several primary light isotopes act as major neutron absorbers at low metallicity. Their cross sections often show large departures from the $1/v$ law and, therefore, need to be carefully evaluated. Among them are ^{12}C, ^{16}O, ^{20}Ne, and all Si isotopes (see Bao et al. 2000). Of particular importance for the *s*-process efficiency is ^{16}O, for which Igashira et al. (1995) measured a neutron-capture cross section that turned out to be 170 times higher than previous theoretical estimates by Allen & Macklin (1971). As a matter of fact, even employing the much lower value from Allen & Macklin (1971), the neutron capture on ^{16}O in massive stars was found to strongly depress the weak *s*-process at low metallicity (Raiteri et al. 1992). The effect may be moderated by the partial recycling effect of the chain ^{16}O$(n, \gamma)^{17}$O$(\alpha, n)^{20}$Ne (Travaglio et al. 1996). Recently, Woosley et al. (2003) noted the importance of including the effect of neutron poisoning from ^{16}O in core-collapse supernovae of solar metallicity.

Besides all of the above intricacies, a major impact is played by the need for a careful knowledge of key reaction rates, like ^{22}Ne$(\alpha, n)^{25}$Mg and ^{22}Ne$(\alpha, \gamma)^{26}$Mg (Käppeler et al. 1994; see Rauscher et al. 2002; Woosley et al. 2003). One has finally to recall the critical effect on the advanced phases of stellar evolution and nucleosynthesis that results from the choice for the important, but uncertain, ^{12}C$(\alpha, \gamma)^{16}$O reaction rate (see Rauscher et al. 2002 for a recent discussion). Other difficulties are related to a realistic treatment of convective-radiative borders, the time-dependent mixing and nucleosynthesis processes, the inclusion of rotation and mass loss, and hydrodynamic multidimensional effects.

In spite of the above-mentioned problems affecting neutron-capture nucleosynthesis in massive stars and the nucleosynthetic origin of the *r*-process, a general conclusion may be drawn. Because of the metallicity dependence of the major neutron source, ^{22}Ne, no contribution from the weak *s*-process is to be expected in halo stars. Some extra contribution is, however, to be expected from primary neutron sources in massive stars, whose quantitative impact is difficult to determine at present.

5.3. *Primary Neutron-Capture Sources in Massive Stars not Related to the Classical r-Process*

In the more advanced evolutionary stages of massive stars there are a few primary neutron sources that may be activated, among which is the possible contribution during carbon burning of the subthreshold channel $^{12}\mathrm{C} + ^{12}\mathrm{C} \rightarrow ^{23}\mathrm{Mg} + n$ (Caughlan & Fowler 1988). Another important source of neutrons during C burning is the reaction ^{26}Mg$(\alpha, n)^{29}$Si, where ^{26}Mg is partly of primary origin from the chain $^{12}\mathrm{C} + ^{12}\mathrm{C} \rightarrow ^{23}\mathrm{Na} + p$ followed by ^{23}Na$(\alpha, p)^{26}$Mg. In the subsequent hydrostatic O-burning phase, which takes place at around 2×10^9 K, an intense primary neutron production is released by the reaction channel $^{16}\mathrm{O} + ^{16}\mathrm{O} \rightarrow ^{31}\mathrm{S} + n$. Explosive nucleosynthesis governs the yields of the ejecta of the Si-rich zone and of the inner region of the O-rich zone, where photodisintegration processes on heavy isotopes play a consistent role on dynamical timescales. In the postexplosive nucleosynthesis yields of massive stars with solar composition (Rauscher et al. 2002), with an expected sharp decline for nuclides beyond the neutron magic $N = 50$, there are comparable amounts of *r*-only and *s*-only isotopes, ^{70}Zn and ^{70}Ge, ^{76}Ge and ^{76}Se, ^{80}Se and ^{80}Kr, ^{82}Se and ^{82}Kr, ^{86}Sr and ^{86}Kr, which is impossible to explain either by the weak *s*-process or by a pure *r*-process mechanism.

These first detailed results for the buildup of heavy elements with a full reaction network in core-collapse supernovae are reminiscent of the older numerical simulations aimed at characterizing the astrophysical site for the nucleosynthesis of the *r*-process. For example, simulations of neutron captures occurring after the passage of a shock front at explosive He shell conditions ($\rho \lesssim 10^5$ g cm^{-3}, 0.9×10^9 K $\lesssim T \lesssim 2 \times 10^9$ K) were able to reproduce only the *r*-process peak at $A = 80$ (Hillebrandt, Kodama, & Takahashi 1976; Hillebrandt & Thielemann 1977; Truran, Cowan, & Cameron 1978; Cowan, Cameron, & Truran 1985). That result was considered a failure in the quest for a common astrophysical site for reproducing the whole *r*-process distribution in the solar system, from $A \sim 80$ up to the transuranics. Nevertheless, the growth of spectroscopic data now available suggests that neither the *s*-process nor the *r*-process in nature is the result of unique nucleosynthesis processes.

5.4. *The r-Process Contribution to* Sr, Y, Zr *as Deduced from Very Metal-poor and Very r-Process–rich Stars*

As briefly described in § 3.2, our estimate of *r*-process abundances for the elements from Ba to Pb at $t = t_\odot$ has been derived using the *r*-process residuals method. If we would

apply the same method to Sr-Y-Zr, we would obtain an *r*-process contribution of ~20%–30% to the solar composition (see Table 3). Nevertheless, the more complex nucleosynthetic origin of the Sr-Y-Zr elements with respect to the Ba–Eu elements is suggested by *r*-process–rich and very low metallicity stars, such as CS 22892−052. Since this star has an *r*-process enrichment of ~40 times the solar-scaled composition (see Fig. 5, [Eu/Fe] versus [Fe/H], *middle panel*), we can ascribe the signature of CS 22892−052 to the "pure" *r*-process (i.e., any contamination by other possible stellar sources is hidden by the *r*-process abundances). A very similar trend in both Sr-Y-Zr and the heavy elements beyond Ba is shown by another very *r*-process–rich star of nearly the same metallicity, e.g., CS 31081−001. Both CS 22892−052 and CS 31081−001 are highlighted as bold symbols in the various figures. In particular, these two stars show the highest [Sr/Fe], [Y/Fe], and [Zr/Fe] ratios among stars of comparable metallicity (see Fig. 4). The other special stars, indicated as open circles, for which accurate spectroscopic abundances of many neutron-capture elements are available, do not show such an extreme *r*-process–rich signature. For them, both Sr, Y, Zr and Ba, Eu cannot be distinguished from the averages of other stars of comparable metallicity.

Under the above assumption, and knowing that the Ba *r*-fraction at the epoch of the solar system formation is ~20% (Travaglio et al. 1999; Arlandini et al. 1999), from CS 22892−052 one can derive the *r*-fraction for Sr-Y-Zr of ~10% (and *not* ~25%–30% as derived from the *r*-residuals method). Note that the same result can be obtained employing Eu instead of Ba. In addition, as noted above, we know that the *s*-process contributes 80%, 74%, and 67% to solar Sr, Y, and Zr, respectively (see Table 4, second column).

After summing up all these contributions, we find that fractions of 8%, 18%, and 18% of solar Sr, Y, and Zr, respectively, are "missed." We then assume that this missing fraction is of "primary" origin and results from all massive stars. We note that at this time it is not possible to completely define this additional nucleosynthetic contribution to Sr, Y, and Zr. In the advanced stages of evolution in massive stars, and in particular during explosive oxygen burning, a number of "primary" neutron sources can be activated. The situation is complicated, however, and neutron production might also be accompanied by photodisintegrations, as well as by proton and α-captures. It appears that this nucleosynthesis is only contributing to the production of the lighter *n*-capture elements (Sr–Zr)—although the production of all elements from Cu to Zr could be affected—and this is of a primary nature. For ease of discussion we would label this additional nucleosynthesis as a lighter element primary process (LEPP). We emphasize further that detailed (full network) supernova model calculations, for stars of low metallicity (as opposed to solar-metallicity models), are not yet available but will be required to better understand this nucleosynthesis. Additional observational data, particularly for Sr-Y-Zr in low-metallicity stars, will also help to constrain theoretical models and better define the nature of lighter *n*-capture element synthesis in low-metallicity stars. The fractional contributions to Sr-Y-Zr from this LEPP are reported in the last column of Table 4. In Table 4 (third column) we also report for comparison purposes the *r*-fraction obtained with the *r*-residuals method. In the case of Nb, since its abundance results from the radiogenic decay of ^{93}Zr, we have adopted the same contribution estimated for Zr. Therefore, knowing its total *s*-process contribution to solar Nb, we have deduced the *r*-fraction without relying on the still uncertain observed value of [Nb/Fe]. We also warn the reader on the Mo *r*-fraction derived from the same star, as a result of difficulties in detecting Mo in low-metallicity stars (see discussion in Sneden et al. 2003, where the error bar for the Mo abundance in CS 22892−052 has been estimated to be ~0.2 dex).

In Table 5 we derive from CS 22892−052 the *r*-fraction of elements from Ru to Cd strictly based on the production of the heavy *r*-elements beyond Ba. In the case of Ru a *p*-process contribution (to ^{96}Ru and ^{98}Ru) has been taken into account, affecting the solar Ru by ~7%. These elements are not the subject of this work; therefore, we will not enter into a detailed discussion here. Since Cd in CS 22892−052 is an upper limit, we report in parentheses the *r*-fraction derived for that element in this star.

The discrepancy in the *r*-fraction of Sr-Y-Zr between the *r*-residuals method and the CS 22892−052 abundances becomes even larger for elements from Ru to Cd: the weak *s*-process does not contribute to elements from Ru to Cd. As noted in the introduction, this discrepancy suggests an even more complex multisource nucleosynthetic origin for elements like Ru, Rh, Pd, Ag, and Cd.

In Figure 9 the *n*-capture abundance pattern observed in the ultra–metal-poor star CS 22892−052 is compared with the *r*-process abundance curve obtained by computing the GCE of *s*-process nucleosynthesis from AGB stars and using the *r*-process residuals method to infer the *r*-process fractions. Exceptions are the *r*-process contributions to Sr, Y, Zr, Nb, and Mo, for which we derived the *r*-process fraction from CS 22892−052. The values plotted in Figure 9 correspond to the ones reported in the fourth column of Table 4. Even when we derived the *r*-fraction for Sr, Y, Zr, Nb, and Mo from CS 22892−052, small differences between our theoretical prediction and the observational data are still visible. This is due to observational uncertainties affecting the data (e.g., deriving the *r*-fraction using Eu instead of Ba will result in differences up to 5% for the elements from Sr to Mo).

TABLE 4

s-Process Contribution and *r*-Process Fraction at the Solar Composition

Element	*s*-Fraction AGB+weak *s* (%)	*r*-Fraction		*n*-Fraction (%)
		r-Residuals (%)	From CS 22892−052 (%)	
Sr	80	20	12	8
Y	74	26	8	18
Zr	67	33	15	18
Nb	69	31	13	18
Mo	39	37	12	25

TABLE 5

s-Process Contribution and *r*-Process Fraction at the Solar Composition for Elements from Ru to Cd

Element	*s*-Fraction AGB+weak *s* (%)	*r*-Fraction	
		r-Residuals (%)	From CS 22892−052 (%)
Ru.....	24	69	50
Rh.....	10	90	43
Pd	36	64	36
Ag.....	9	91	30
Cd.....	38	62	(41)

Spectroscopic data of the elemental abundances in CS 22892−052 (Sneden et al. 2003) plotted in Figure 9 are the result of an average between ground-based observations and *Hubble Space Telescope* (*HST*) observations (with the exception of Pb). For Pb both ground-based and *HST* data have been plotted. For Au no ground-based data are available; therefore, only *HST* data have been plotted. Except for Pb, all *HST* data (Ge, Y, Os, Pt, Au, Pb) seem to be consistent with the ground-based data. Concerning Pb, the uncertainties are still significant even in the ground-based data, as Sneden et al. (2003) commented in their work ". . . we are not confident of the suggested detections of two Pb I lines in the ground-based spectra." We note that for Nb and Mo the observational error bars plotted are "adopted error bars" (see Sneden et al. 2003 for discussion). We also added error bars to our theoretical GCE predictions. They are based, for each isotope, on uncertainties in the solar system elemental abundances (Anders & Grevesse 1989) and on the uncertainties in neutron-capture cross sections (Bao et al. 2000). These error bars are important for elements belonging to the three *s*-peaks, and in particular for Pb. In the case of La, we have adopted a conservative 2 σ uncertainty, since discrepant experimental determinations of the neutron cross section are reported in the compilation of Bao et al. (2000).

6. RECONSTRUCTION OF THE GALACTIC EVOLUTION OF Sr, Y, AND Zr, BY DIVERSE NEUTRON-CAPTURE MECHANISMS

In Figure 10 we show the Galactic evolutionary trends predicted by our model for [Sr/Fe], [Y/Fe], [Zr/Fe] versus [Fe/H].

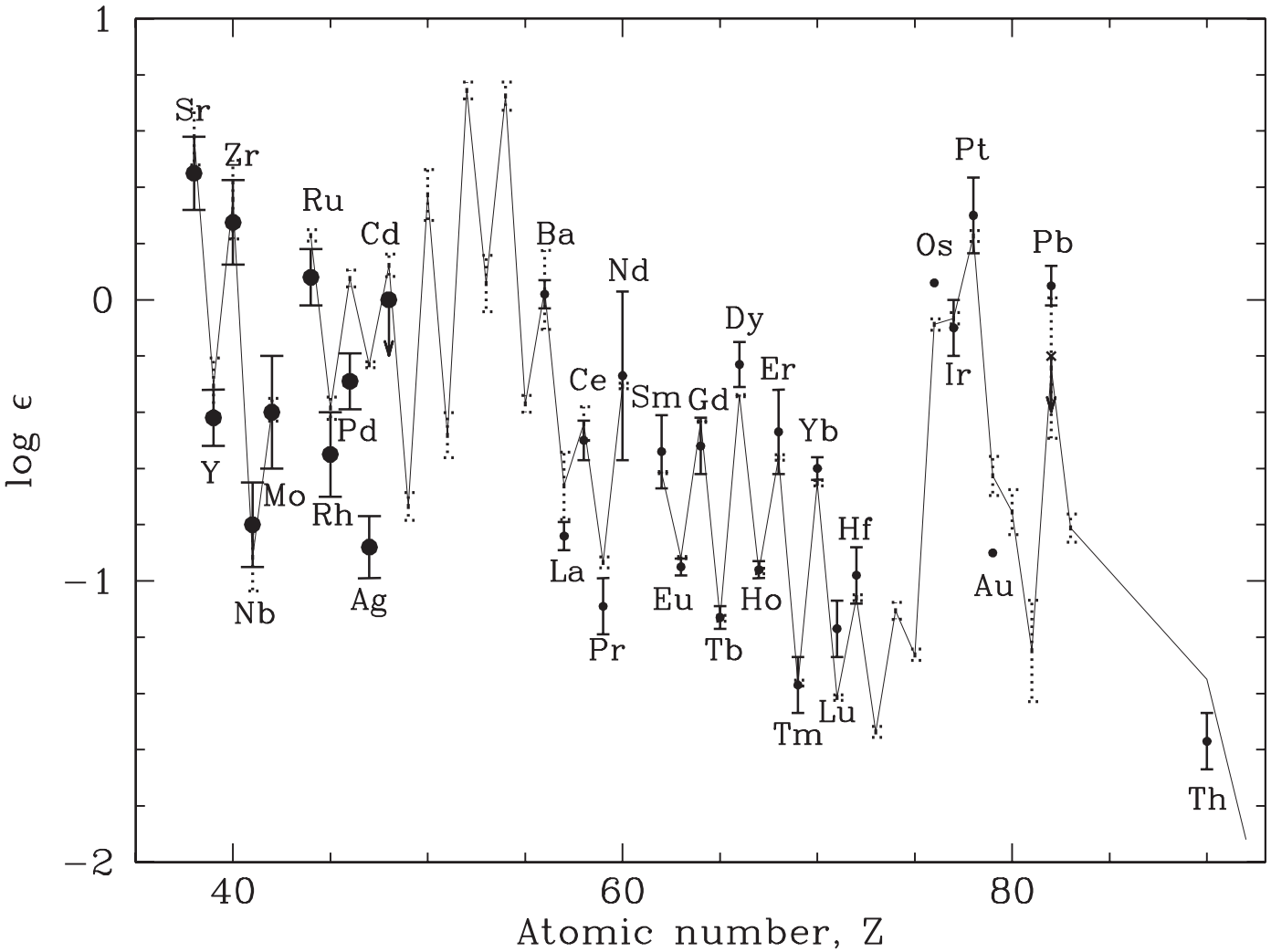

Fig. 9.—Neutron-capture elements observed in CS 22892−052. Ground-based and *HST* data (see text) are taken into account. For Pb, the *HST* measurement (upper limit) has been plotted as a cross. Observations are compared to a scaled abundance curve (*long-dashed lines*) obtained with GCE calculations described in the text. Theoretical error bars are also plotted with dotted lines.

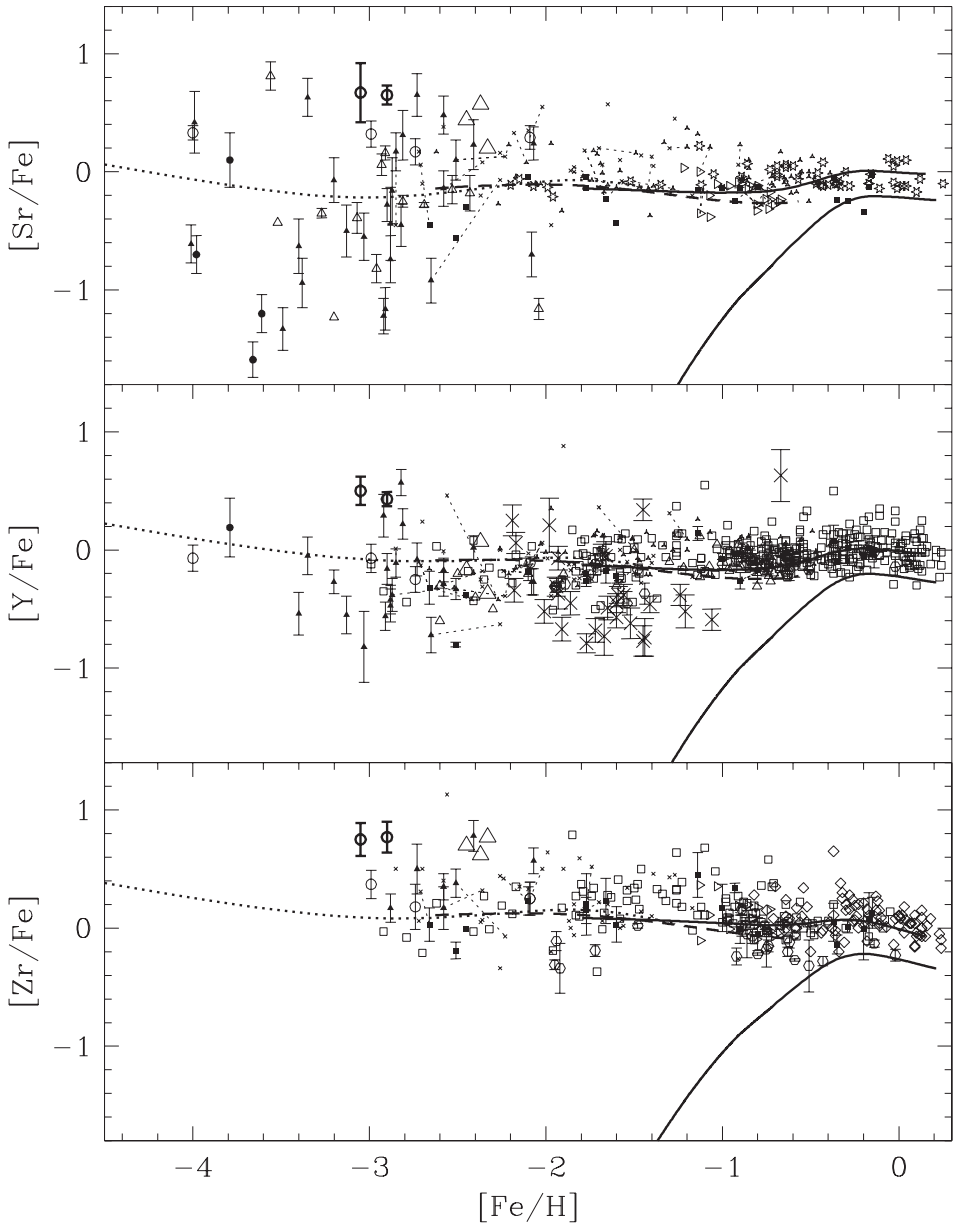

FIG. 10.—Galactic evolution of [Sr/Fe] (*top*), [Y/Fe] (*middle*), and [Zr/Fe] (*bottom*) vs. [Fe/H], according to our model predictions for the *s*-process, and the total (*s*+*r*+primary-process), in the halo (*dotted lines*), thick disk (*dashed lines*), and thin disk (*solid lines*). Observational data (*open circles*) have been discussed in § 4 and shown in Fig. 4.

These predictions take into account the *s*-process, the *r*-process, and the primary process (or LEPP), in the halo, thick disk, and thin disk. In Figure 10 also the GCE model predictions for the *s*-process contribution by AGB stars alone are reported. For Galactic disk metallicities, in the predicted total (*s*+*r*+*primary*) average trend one can distinguish the effect of the late AGB contribution and also a tiny difference in the relative behavior of Sr, Y, and Zr at [Fe/H] > -0.3. It is tempting to interpret in this manner the different trends observed in [Zr/Fe] and [Y/Fe] in disk metallicity stars as described in the introduction. However, a more detailed analysis would be needed when comparing results of different authors in order to distinguish intrinsic abundance variations from observational uncertainties.

In Figure 11 we show the predicted trends for [Sr/Y], [Sr/Zr], and [Y/Zr] versus [Fe/H], and in Figure 12 we show the predicted trends for [Sr/Ba], [Y/Ba], and [Zr/Ba] versus [Fe/H]. In particular, we focus on the ratio of Sr, Y, Zr over Ba for the following reason. Ba, as discussed previously, at low metallicity is mainly produced by *r*-process nucleosynthesis. *If* Ba and Sr-Y-Zr would derive from the same stellar source at such low metallicities, we would expect to see a fairly flat ratio versus [Fe/H] (within observational error bars), as in the case of [Ba/Eu] (see Travaglio et al. 1999 for further discussion). This does not seem to be the case for Sr-Y-Zr, suggesting a different stellar origin for Sr-Y-Zr and Ba.

At very low metallicity the increasing [Sr, Y, Zr/Ba] ratio with decreasing [Fe/H] is correlated with the delayed production of Ba with respect to Sr-Y-Zr. This assumes that at low metallicity Ba is produced in Type II supernovae in the mass range 8–10 $M_{\odot}$, while Sr-Y-Zr derive their *n*-component from all massive stars. The *r*-fraction alone is shown in Figure 12 by a flat line in the three panels, which is consistent with the values for the two extremely *r*-process–rich stars CS 22892−052 and CS 31082−001.

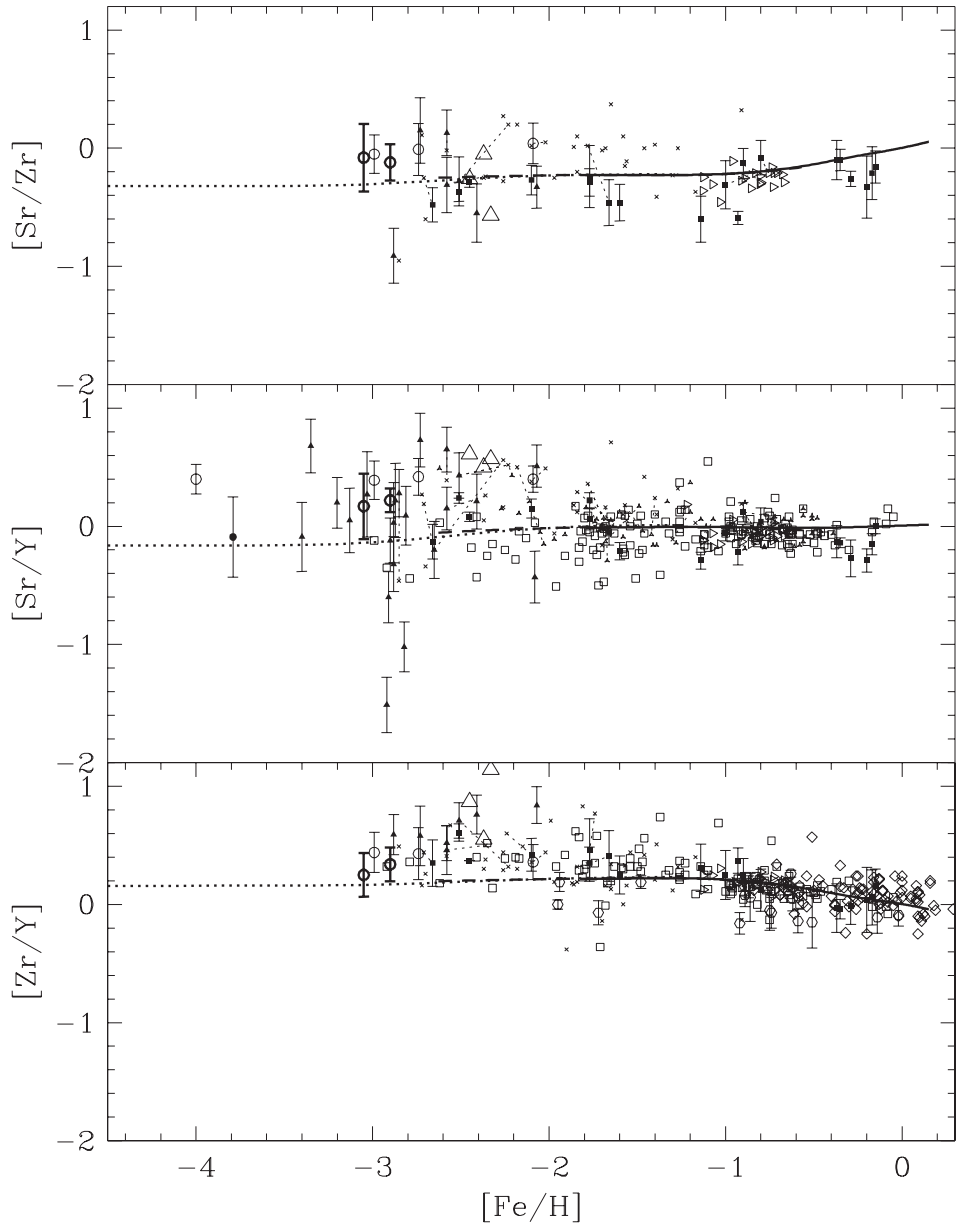

FIG. 11.—Same as Fig. 10, but for [Sr/Zr] (*top*), [Sr/Y] (*middle*), and [Zr/Y] (*bottom*) vs. [Fe/H]. The curves represent the total *s*+*r*+primary contribution for the halo (*dotted lines*), thick disk (*dashed lines*), and thin disk (*solid lines*).

There have been recent observations of *n*-capture elements in nearby dwarf spheroidal galaxies (Shetrone et al. 2001, 2003). Abundance comparisons in these galaxies, as a function of metallicity, demonstrate similar patterns to those observed in the Galaxy. From the Shetrone et al. (2001, 2003) data for Ba and Eu (our Fig. 5) we note that the abundance scatter present in [Ba/Fe] and [Eu/Fe] for $[Fe/H] < -1.5$ disappears at increasing metallicities, in a manner similar to the Galactic sample. Such an agreement among these various galaxies suggests a common synthesis history for these elements as a function of iron production. Nevertheless, the [Y/Fe] in dwarf galaxy stars with $-2 < [Fe/H] < -1$ seems on average lower than what is observed in the Galaxy (Figs. 4 and 10). The same is true for the ratio [Y/Ba] (Figs. 7 and 12). Of course, the stellar sample in dwarf galaxies is still too low to draw any final conclusions. Moreover, no data for Sr and Zr are available, and different star formation histories for each dwarf galaxy should be carefully taken into account (Tolstoy et al. 2003). In spite of these intricacies, one possible explanation for the observed lower [Y/Fe] and [Y/Ba] ratios in dSph galaxies is that less ejecta from massive stars are retained in the local interstellar medium, consequently reducing the contribution to Y from a primary process (see discussion in this paper). Summing up, an increase in the small number statistics of stars observed in dSph galaxies, as well as additional data for Sr and Zr in dSph stars, will allow us to better understand the nucleosynthesis history in these galaxies.

7. CONCLUSIONS

In this paper we have calculated the evolution of the light *n*-capture elements, Sr, Y, and Zr. The input stellar yields for these nuclei have been separated into their *s*-, *r*-, and primary-process components. The *s*-yields are the result of postprocess nucleosynthesis calculations based on full

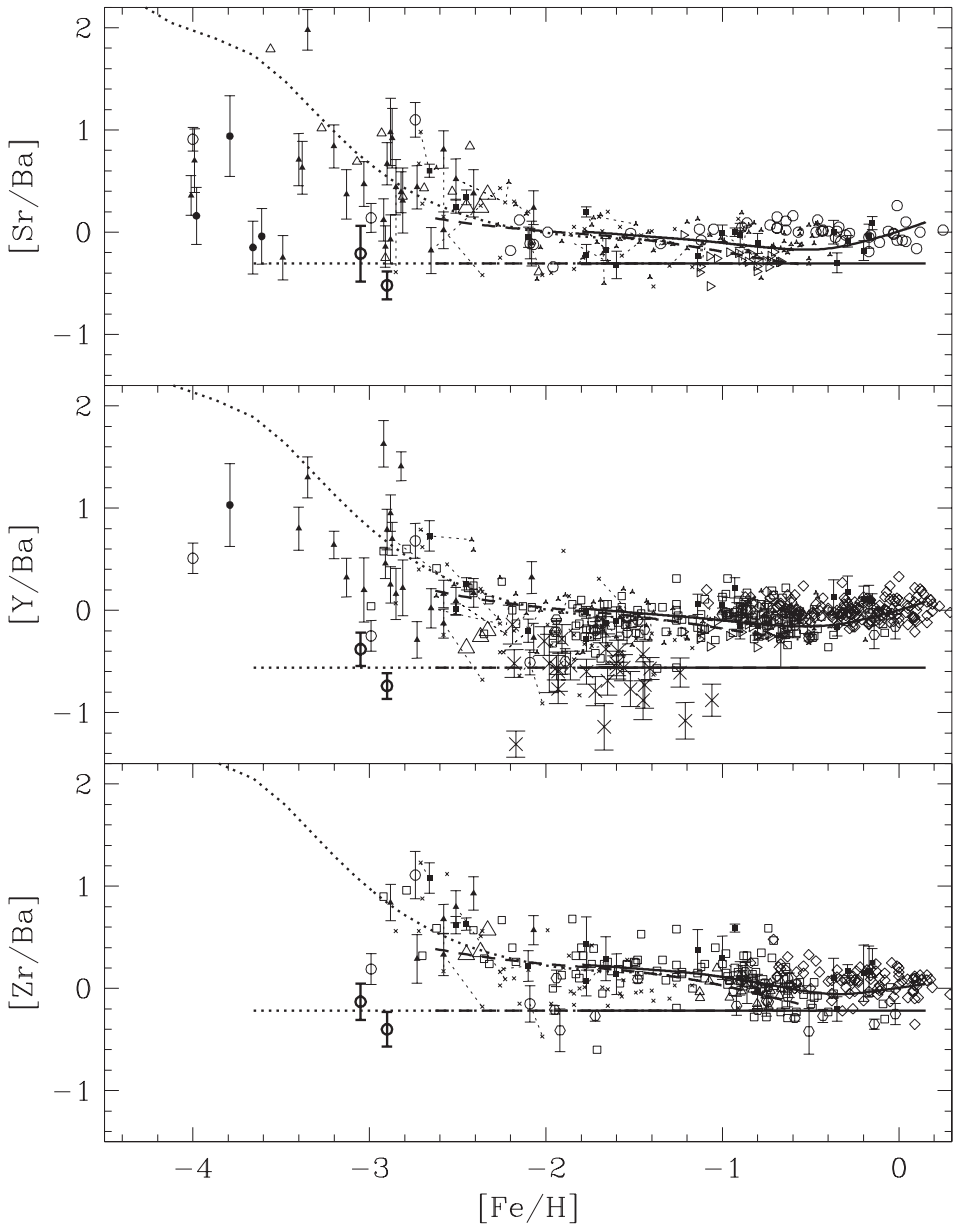

FIG. 12.—Same as Fig. 10, but for [Sr/Ba] (*top*), [Y/Ba] (*middle*), and [Zr/Ba] (*bottom*) vs. [Fe/H] for the halo (*dotted lines*), thick disk (*dashed lines*), and thin disk (*solid lines*). With thick lines the *r*-process contribution alone is also plotted for comparison.

evolutionary AGB models computed with FRANEC. Spectroscopic observations of very low metallicity stars in the Galaxy, as well as the first observations of single stars in dwarf spheroidal galaxies, suggest that an extra source (of primary nature) is needed to synthesize Sr, Y, and Zr, to enrich the early interstellar medium, and to reproduce the solar composition of *s*-only isotopes like ^{86}Sr, ^{87}Sr, and ^{96}Mo. We therefore think that neutrons should give the major imprint to this primary process, which has to be considered different from the classical *s*- and the classical *r*-processes. The results of the Galactic evolution model confirm these observational indications.

We compared our theoretical predictions with the abundance pattern observed in the very *r*-process–rich CS 22892−052 (Sneden et al. 2003). This star is known to show a *pure r*-process signature (it shows an *r*-process enhancement of about 40 times the solar value, much larger than any abundance observed in normal halo stars). We extracted from this star the *r*-fraction of Sr, Y, and Zr (∼10% of the solar value). In the light of our nucleosynthesis calculations in AGB stars at different metallicities, integrated over the GCE model briefly described in this paper, we conclude that the *s*-process from AGB stars contributes to the solar abundances of Sr, Y, and Zr by 71%, 69%, and 65%, respectively. To the solar Sr abundance, we also added a small contribution (∼10%) from the "secondary" weak *s*-component from massive stars.

As a consequence of the above results, we conclude that a primary component from massive stars is needed to explain 8% of the solar abundance of Sr and 18% of solar Y and Zr. Although this contribution to the solar composition is small, especially in terms of the overall uncertainties, it nevertheless appears to be necessary to produce the observed enrichment of these elements in the very low metallicity stars. This process is of *primary* nature, unrelated to the classical metallicity-dependent weak *s*-component, and might be

thought of as an LEPP. We stress that the details of this nucleosynthesis are still not well understood, and charged-particle reactions and photodisintegrations may contribute along with neutron production. Further, the same process to which the light neutron-capture elements Sr, Y, and Zr are sensitive also likely affects the production of all elements from Cu to Sr. To understand in detail the complicated Galactic nucleosynthesis history of Sr, Y, and Zr (as well as other lighter element) formation will require new theoretical studies and additional high-quality spectroscopic observational data, particularly of low-metallicity halo stars.

C. T. thanks the Alexander von Humboldt Foundation, the Federal Ministry of Education and Research, and the Programme for Investment in the Future (ZIP) of the German Government for their financial support. R. G. thanks Max-Planck-Institut für Cosmochemie (Mainz) for the kind hospitality during the development of this work. We thank the anonymous referee for helpful suggestions that have improved the paper. Research was partly supported by the MIUR-FIRB Project "The Astrophysical Origin of Heavy Elements beyond Fe" (C. T., R. G.) and by NSF grants AST 99-86974, AST 03-07279 (J. J. C.), AST 99-87162, and AST 03-07495 (C. S.).

REFERENCES

Abia, C., Busso, M., Gallino, R., Domínguez, I., Straniero, O., & Isern, J. 2001, ApJ, 559, 1117
Abia, C., et al. 2002, ApJ, 579, 817
Allen, B. J., & Macklin, R. L. 1971, Phys. Rev. Lett., 3, 1737
Anders, E., & Grevesse, N. 1989, Geochim. Cosmochim. Acta, 53, 197
Argast, D., Samland, M., Gerhard, O. E., & Thielemann, F.-K. 2000, A&A, 356, 873
Argast, D., Samland, M., Thielemann, F.-K., & Gerhard, O. E. 2002, A&A, 388, 842
Arlandini, C., Käppeler, F., Wisshak, K., Gallino, R., Lugaro, M., Busso, M., & Straniero, O. 1999, ApJ, 525, 886
Arnett, W. D., & Thielemann, F.-K. 1985, ApJ, 295, 589
Arnett, W. D., & Truran, J. W. 1969, ApJ, 157, 339
Arnone, E., Travaglio, C., Gallino. R., & Straniero, O. 2003, in CNO in the Universe, in press
Bao, Z. Y., Beer, H., Käppeler, F., Wisshak, K., & Rauscher, T. 2000, At. Data Nucl. Data Tables, 76, 70
Boldeman, J., Musgrove, A. d. L., Allen, B. J., Harvey, B. J., & Macklin, R. L. 1976, Nucl. Phys. A, 269, 31
Burbidge, E. M., Burbidge, G. R., Fowler, W. A., & Hoyle, F. 1957, Rev. Mod. Phys., 29, 547
Burris, D. L., Pilachowski, C. A., Armandroff, T. E., Sneden, C., Cowan, J. J., & Roe, H. 2000, ApJ, 544, 302
Busso, M., Gallino, R., Lambert, D. L., Travaglio, C., & Smith, V. V. 2001, ApJ, 557, 802
Busso, M., Gallino, R., & Wasserburg, G. J. 1999, ARA&A, 37, 239
Busso, M., Lambert, D. L., Gallino, R., Beglio, L., Raiteri, C. M., & Smith, V. V. 1995, ApJ, 446, 775
Cameron, A. G. W. 1973, Space Sci. Rev., 15, 121
———. 2001, ApJ, 562, 456
———. 2003, ApJ, 587, 327
Caughlan, G. R., & Fowler, W. A. 1988, At. Data Nucl. Data Tables, 40, 283
Cayrel, R., et al. 2001, Nature, 409, 691
Chieffi, A., & Straniero, O. 1989, ApJS, 71, 47
Clayton, D. D., Fowler, W. A., Hull, T. E., & Zimmerman, B. A. 1961, Ann. Phys., 12, 331
Clayton, D. D., & Rassbach, M. E. 1967, ApJ, 148, 69
Clayton, D. D., & Ward, R. A. 1974, ApJ, 192, 501
Couch, R. G., Schmiedekamp, A. B., & Arnett, W. D. 1974, ApJ, 190, 95
Cowan, J. J., Cameron, A. G. W., & Truran, J. W. 1985, ApJ, 294, 656
Cowan, J. J., et al. 2002, ApJ, 572, 861
Cristallo, S., Straniero, O., Gallino, R., Herwig, F., Chieffi, A., Limongi, M., & Busso, M. 2001, Nucl. Phys. A, 688, 217
Depagne, E., et al. 2002, A&A, 390, 187
Duncan, R. C., Shapiro, S. L., & Wasserman, I. 1986, ApJ, 309, 141
Edvardsson, B., Andersen, J., Gustafsson, B., Lambert, D., Nissen, P. E., & Tomkin, J. 1993, A&AS, 102, 603
Ferrini, F., Matteucci, F., Pardi, C., & Penco, U. 1992, ApJ, 387, 138
Freiburghaus, C., Rembges, J. F., Rauscher, T., Kolbe, E., Thielemann, F.-K., Kratz, K. L., Pfeiffer, B., & Cowan, J. 1999, ApJ, 516, 381
Fulbright, J. P. 2000, AJ, 120, 1841
Galli, D., Palla, F., Ferrini, F., & Penco, U. 1995, ApJ, 443, 536
Gallino, R., Arlandini, C., Busso, M., Lugaro, M., Travaglio, C., Straniero, O., Chieffi, A., & Limongi, M. 1998, ApJ, 497, 388
Gilroy, K. K., Sneden, C., Pilachowski, C. A., & Cowan, J. J. 1988, ApJ, 327, 298
Gratton, R. G., & Sneden, C. 1988, A&A, 204, 193
———. 1994, A&A, 287, 927
Griffin, R., Gustaffsson, B., Vieira, T., & Griffin, R. 1982, MNRAS, 198, 637
Heger, A., & Woosley, S. E. 2002, ApJ, 567, 532
Heger, A., Woosley, S. E., Martinez-Pinedo, G., & Langanke, K. 2001, ApJ, 560, 307
Herwig, F., Blöcker, T., Schönberner, D., & El Eid, M. 1997, A&A, 324, L81
Hill, V., et al. 2002, A&A, 387, 560
Hillebrandt, W. 1978, Space Sci. Rev., 21, 639
Hillebrandt, W., Kodama, T., & Takahashi, K. 1976, A&A, 52, 63
Hillebrandt, W., & Thielemann, F. K. 1977, A&A, 58, 357
Hoffman, R. D., Woosley, S. E., & Weaver, T. A. 2001, ApJ, 549, 1085
Hollowell, D. E., & Iben, I., Jr. 1988, ApJ, 333, L25
Iben, I., Jr. 1975, ApJ, 196, 525
Igashira, M., Nagai, Y., Masuda, K., Ohsaki, T., & Kitazawa, H. 1995, ApJ, 441, L89
Ikuta, C., & Arimoto, N. 1999, PASJ, 51, 459
Ivans, I. I., Kraft, R. P., Sneden, C., Smith, G. H., Rich, R. M., & Shetrone, M. D. 2001, AJ, 122, 1438
Ivans, I. I., Sneden, C., Kraft, R. P., Suntzeff, N. B., Smith, V. V., Langer, G. E., & Fulbright, J. P. 1999, AJ, 118, 1273
Jehin, E., Magain, P., Neuforge, C., Noels, A., Parmentier, G., & Thoul, A. A. 1999, A&A, 341, 241
Johnson, J. A., & Bolte, M. 2002, ApJ, 579, 616
Käppeler, F., Beer, H., & Wisshak, K. 1989, Rep. Prog. Phys., 52, 945
Käppeler, F., Beer, H., Wisshak, K., Clayton, D. D., Macklin, R. L., & Ward, R. A. 1982, ApJ, 257, 821
Käppeler, F., Gallino, R., Busso, M., & Raiteri, C. M. 1990, ApJ, 354, 630
Käppeler, F., et al. 1994, ApJ, 437, 396
Koehler, P. E., et al. 2000, Phys. Rev. C, 62, 055803
Lamb, S., Howard, W. M., Truran, J. W., & Iben, I., Jr. 1977, ApJ, 217, 213
Langer, N., Heger, A., Wellstein, S., & Herwig, F. 1999, A&A, 346, L37
Leblanc, J., & Wilson, J. R. 1970, ApJ, 161, 541
Limongi, M., & Chieffi, A. 2003, ApJ, 592, 404
Lugaro, M., Davis, A. M., Gallino, R., Pellin, M. J., Straniero, O., & Käppeler, F. 2003, ApJ, 593, 486
Lugaro, M., Zinner, E., Gallino, R., & Amari, S. 1999, ApJ, 527, 369
Mashonkina, L., & Gehren, T. 2001, A&A, 376, 232
Mathews, G. J., & Cowan, J. J. 1990, Nature, 345, 491
Matteucci, F., Raiteri, C. M., Busso, M., Gallino, R., & Gratton, R. 1993, A&A, 272, 421
McWilliam, A. 1998, AJ, 115, 1640
McWilliam, A., Preston, G. W., Sneden, C., & Searle, L. 1995, AJ, 109, 2736
Mishenina, T. V., & Kovtyukh, V. V. 2001, A&A, 370, 951
Mishenina, T. V., Kovtyukh, V. V., Soubiran, C., Travaglio, C., & Busso, M. 2002, A&A, 396, 189
Norris, J. E., Ryan, S. G., & Beers, T. C. 2001, ApJ, 561, 1034
Prantzos, N., Hashimoto, M., Rayet, M., & Arnould, M. 1990, A&A, 238, 455
Qian, Y. Z. 2000, ApJ, 534, L67
Qian, Y. Z., & Wasserburg, G. J. 2001, ApJ, 559, 925
Raiteri, C. M., Busso, M., Gallino, R., & Picchio, G. 1991a, ApJ, 371, 665
Raiteri, C. M., Busso, M., Gallino, R., Picchio, G., & Pulone, L. 1991b, ApJ, 367, 228
Raiteri, C. M., Gallino, R., & Busso, M. 1992, ApJ, 387, 263
Raiteri, C. M., Gallino, R., Busso, M., Neuberger, D., & Käppeler, F. 1993, ApJ, 419, 207
Raiteri, C. M., Villata, M., Gallino, R., Busso, M., & Cravanzola, A. 1999, ApJ, 518, L91
Rauscher, T., Heger, A., Hoffman, R. D., & Woosley, S. E. 2002, ApJ, 576, 323
Ryan, S. G., Norris, J. E., & Beers, T. C. 1996, ApJ, 471, 254
Ryan, S. G., Norris, J. E., & Bessel, M. S. 1991, AJ, 102, 303
Seeger, P. A., Fowler, W. A., & Clayton, D. D. 1965, ApJS, 11, 121
Shetrone, M. D., Côté, P., & Sargent, W. L. W. 2001, ApJ, 548, 592
Shetrone, M. D., Venn, K. A., Tolstoy, E., Primas, F., Hill, V., & Kaufer, A. 2003, AJ, 125, 684
Simmerer, J., Sneden, C., Ivans, I., Kraft, R. P., Shetrone, M. D., & Smith, V. V. 2003, AJ, 125, 2018
Sneden, C., Cowan, J. J., Burris, D. L., & Truran, J. W. 1998, ApJ, 496, 235

Sneden, C., Cowan, J. J., Ivans, I. I., Fuller, G. M., Burles, S., Beers, T. C., & Lawler, J. E. 2000a, ApJ, 533, L139
Sneden, C., Johnson, J., Kraft, R. P., Smith, G. H., Cowan, J. J., & Bolte, M. S. 2000b, ApJ, 536, L85
Sneden, C., Kraft, R. P., Shetrone, M. D., Smith, G. H., Langer, G. E., & Prosser, C. F. 1997, AJ, 114, 1964
Sneden, C., et al. 2003, ApJ, 591, 936
Spite, M., & Spite, F. 1978, A&A, 67, 23
Straniero, O., Chieffi, A., Limongi, M., Busso, M., Gallino, R., & Arlandini, C. 1997, ApJ, 478, 332
Straniero, O., Gallino, R., Busso, M., Chieffi, A., Raiteri, C. M., Salaris, M., & Limongi, M. 1995, ApJ, 440, L85
Takahashi, K., Witti, J., & Janka, H.-Th. 1994, A&A, 286, 857
Talbot, R. J. J., & Arnett, W. D. 1973, ApJ, 186, 51
The, L.-S., El Eid, M. F., & Meyer, B. S. 2000, ApJ, 533, 998
Thielemann, F. K., & Arnett, W. D. 1985, ApJ, 295, 604
Thomson, T. A., Burrows, A., & Meyer, B. S. 2001, ApJ, 562, 887
Tolstoy, E., Venn, K., Shetrone, M., Primas, F., Hill, V., Kaufer, A., & Szeifert, T. 2003, AJ, 125, 707
Tomkin, J., & Lambert, D. L. 1999, ApJ, 523, 234
Toukan, K., & Käppeler, F. 1990, ApJ, 348, 357
Travaglio, C., Galli, D., & Burkert, A. 2001a, ApJ, 547, 217
Travaglio, C., Galli, D., Gallino, R., Busso, M., Ferrini, F., & Straniero, O. 1999, ApJ, 521, 691
Travaglio, C., Gallino, R., Arlandini, C., & Busso, M. 1996, Mem. Soc. Astron. Italiana, 67, 831
Travaglio, C., Gallino, R., Busso, M., & Gratton, R. 2001b, ApJ, 549, 346
Travaglio, C., Randich, S., Galli, D., Lattanzio, J., Elliott, L. M., Forestini, M., & Ferrini, F. 2001c, ApJ, 559, 909
Truran, J. W. 1981, A&A, 97, 391
Truran, J. W., Cowan, J. J., & Cameron, A. G. W. 1978, ApJ, 222, L63
Truran, J. W., & Iben, I., Jr. 1977, ApJ, 216, 797
Tsujimoto, T., Shigeyama, T., & Yoshii, Y. 1999, ApJ, 519, L63
Wasserburg, G. J., Busso, M., & Gallino, R. 1996, ApJ, 466, L109
Westin, J., Sneden, C., Gustafsson, B., & Cowan, J. J. 2000, ApJ, 530, 783
Wheeler, J. C., Cowan, J. J., & Hillebrandt, W. 1998, ApJ, 493, L101
Woosley, S. E., Heger, A., Rauscher, T., & Hoffmanm, R. D. 2003, Nucl. Phys. A, 518, 73
Woosley, S. E., Heger, A., & Weaver, T. A. 2002, Rev. Mod. Phys., 74, 1015
Woosley, S. E., Wilson, J. R., Mathews, G. J., Hoffman, R. D., & Meyer, B. S. 1994, ApJ, 433, 229